AD-A212 090 MODEL TESTS IN ICE OF A CANADIAN COAST GUARD R-CLASS 1/1
ICEBREAKER - HIGH FR..(U) COLD REGIONS RESEARCH AND
ENGINEERING LAB HANOVER NH J TATINCLAUX ET AL. JUL 89
UNCLASSIFIED CRREL-SR-89-25 F/G 13/10 NL

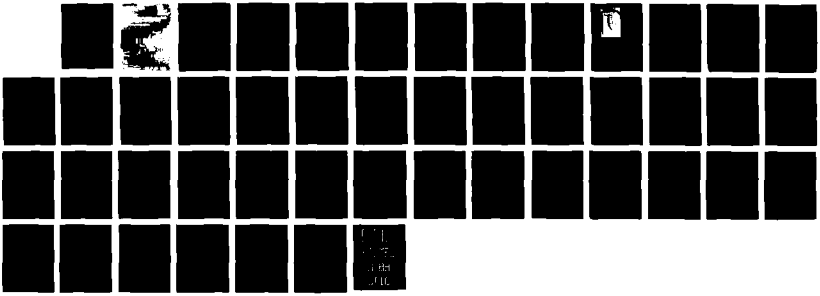

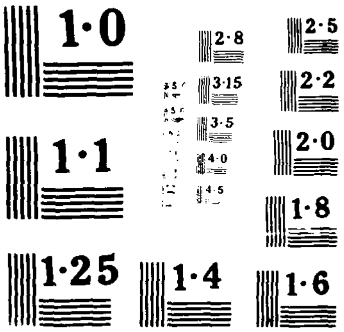
1·0
2·8
2·5
3·15
2·2
3·5
2·0
4·0
1·1
4·5
1·8
1·25
1·4
1·6

UNCLASSIFIED
SECURITY CLASSIFICATION OF THIS PAGE

REPORT DOCUMENTATION PAGE

Form Approved
OMB NO 0704-0188
Exp Date Jun 30 1986

1a. REPORT SECURITY CLASSIFICATION
Unclassified

1B. RESTRICTIVE MARKINGS

2a. SECURITY CLASSIFICATION AUTHORITY

2b. DECLASSIFICATION/DOWNGRADING SCHEDULE

3. DISTRIBUTION/AVAILABILITY OF REPORT
Approved for public release; distribution is unlimited.

4. PERFORMING ORGANIZATION REPORT NUMBER(S)
Special Report 89-25

5. MONITORING ORGANIZATION REPORT NUMBER(S)

6a. NAME OF PERFORMING ORGANIZATION
U.S. Army Cold Regions Research
and Engineering Laboratory

6b. OFFICE SYMBOL *(if applicable)*
CECRL

7a. NAME OF MONITORING ORGANIZATION

6c. ADDRESS *(City, State, and ZIP Code)*
72 Lyme Road
Hanover, N.H. 03755-1290

7b. ADDRESS *(City, State, and ZIP Code)*

8a. NAME OF FUNDING/SPONSORING ORGANIZATION

8b. OFFICE SYMBOL *(if applicable)*

9. PROCUREMENT INSTRUMENT IDENTIFICATION NUMBER
In-House Laboratory Independent Research

8c ADDRESS *(City, State, and ZIP Code)*

10. SOURCE OF FUNDING NUMBERS

PROGRAM ELEMENT NO.	PROJECT NO.	TASK NO	WORK UNIT ACCESSION NO

11. TITLE *(Include Security Classification)*
Model tests in ice of a Canadian Coast Guard R-class icebreaker—high friction model

12. PERSONAL AUTHOR(S)
Tatinclaux, Jean-Claude and Martinson, Carl R.

13a. TYPE OF REPORT

13b. TIME COVERED
FROM ________ TO ________

14. DATE OF REPORT *(Year, Month, Day)*
July 1989

15 PAGE COUNT
46

16. SUPPLEMENTARY NOTATION

17. COSATI CODES

FIELD	GROUP	SUB-GROUP

18. SUBJECT TERMS *(Continue on reverse if necessary and identify by block number)*
Icebreaker
Ice resistance
Model tests
Propulsion tests

19. ABSTRACT *(Continue on reverse if necessary and identify by block number)*

This report presents the results of resistance and propulsion tests in level ice of a roughened 1:20 scale model of the Canadian Coast Guard R-class icebreaker. The test conditions were the same as those previously reported for the smooth model. The present test results and those with the smooth model are compared, as are the results obtained at all facilities participating in the comparative study proposed by the Committee on Performance of Ships in Ice-Covered Waters of the International Towing Tank Conference.

20. DISTRIBUTION/AVAILABILITY OF ABSTRACT
☒ UNCLASSIFIED/UNLIMITED ☐ SAME AS RPT. ☐ DTIC USERS

21. ABSTRACT SECURITY CLASSIFICATION
Unclassified

22a. NAME OF RESPONSIBLE INDIVIDUAL
Jean-Claude Tatinclaux

22b. TELEPHONE *(Include Area Code)*
603-646-4100

22c. OFFICE SYMBOL
CECRL-EI

DD FORM 1473, 84 MAR

83 APR edition may be used until exhausted.
All other editions are obsolete.

SECURITY CLASSIFICATION OF THIS PAGE
UNCLASSIFIED

PREFACE

This report was prepared by Dr. Jean-Claude Tatinclaux, Research Hydraulic Engineer, and by Carl R. Martinson, Mechanical Engineering Technician, Ice Engineering Research Branch, Experimental Engineering Division, U.S. Army Cold Regions Research and Engineering Laboratory. This study was CRREL's continuing contribution to an international cooperative research project proposed by the Committee on Performance of Ships in Ice-Covered Waters at the 16th and 17th International Towing Tank Conference. Funding was provided by CRREL's *In-house Laboratory Independent Research* (ILIR) program.

This report was technically reviewed by Dr. Devinder S. Sodhi, CRREL, and Dr. Robert Ettema, University of Iowa, Iowa City, Iowa.

The contents of this report are not to be used for advertising or promotional purposes. Citation of brand names does not constitute an official endorsement or approval of the use of such commercial products.

CONTENTS

ILLUSTRATIONS

TABLES

NOMENCLATURE

B	ship beam
C_n	dimensionless ice strength
D	propeller diameter
f_a	apparent ice–hull friction factor
f_i	ice–hull friction factor
F_n	Froude number based on ice thickness: $V/\sqrt{gh_i}$
g	acceleration of gravity
h_i	ice thickness
h_s	snow thickness
J_a	apparent advance coefficient: V/n_aD
K_q	torque coefficient
K_t	thrust coefficient
n_a	average rate of propeller rotation
N	normal pressure on ice sample during friction test
PD	delivered power
Q_a	average propeller torque
R_i	net resistance in ice: $R_{it} - R_{ow}$
R_{it}	total resistance in level ice
R_{ow}	resistance in ice-free water
R_p	predicted total resistance
R_*	nondimensional resistance
S	sampling rate of data acquisition (milliseconds)
t	thrust deduction coefficient
T	ship draft; also average tangential force on ice sample during friction test
T_a	average propeller thrust
$T_{1,2}$	average load exerted on either load cell during friction tests
T_o	initial tangential force due to ice adhesion
V, v	ship speed
W	weight applied to ice sample during friction tests
W_s	weight of ice sample and sample holder
W_t	total weight: $W+W_s$
ν	Poisson's ratio of ice ($\simeq$ 0.3)
λ	geometric model scale
ρ	water density
ρ_i	ice density
γ	water specific weight
σ_i	ice flexural strength
τ	ice friction stress
τ_o	ice friction stress ascribable to adhesion

Model Tests in Ice of a Canadian Coast Guard R-class Icebreaker—High Friction Model

JEAN-CLAUDE TATINCLAUX AND CARL R. MARTINSON

INTRODUCTION

At the 16th International Towing Tank Conference (ITTC), Leningrad, USSR, 1981, the Committee on Performance of Ships in Ice-Covered Waters (Ice Committee, for short) initiated an international cooperative research program. Under this cooperative program, the participating ice-testing facilities were to conduct a specified test program with the same icebreaker model according to their own testing and data analysis methods (ITTC 1981). Two 1:20 scale models and two 1:40 scale models of the Canadian Coast Guard R-class icebreaker were specially constructed by the National Research Council of Canada and circulated among the participating facilities. The smaller 1:40 scale models were to be tested in resistance only at

- Arctic and Antarctic Research Institute (AARI), Leningrad, USSR.
- Norwegian Technical Institute (NTI), Trondheim, Norway.

while the larger models were to be tested in resistance and propulsion at

- CRREL, Hanover, New Hampshire, USA.
- Hamburgische Schiffbau Versuchsanstalt (HSVA), Hamburg, FRG.
- Japan Ship Research Institute (JSRI), Tokyo, Japan.
- Institute for Marine Dynamics/National Research Council (NRCC), St-Johns, Newfoundland, Canada.
- Wärtsila Arctic Research Center (WARC), Helsinki, Finland.

Resistance and propulsion tests in ice-free water had been made on an earlier 1:40 scale model and previously reported by the National Research Council of Canada (Murdey 1980).

The results of the tests on the original ship models were reported at the 1984 ITTC in Göteborg, Sweden (ITTC 1984). Comparison of the test results from the various facilities showed that under nominally identical conditions of ice thickness, ice strength and ship-model speed, the ice resistance and the propeller thrust and torque of the 1:20 scale model were within 25% of one another. On the other hand, when these test results were extrapolated to full-scale conditions, the predicted resistance, thrust and torque were significantly below available full-scale trial measurements (Edwards et al. 1981, Michailidis and Murdey 1981). The discrepancies between predicted performance and full-scale measurements were attributed to the ice friction factor of the model hull, measured at 0.04 in the average, being much lower than the estimated value of 0.1 for a new icebreaker hull. The ITTC Ice Committee decided to repeat the resistance and propulsion tests with roughened 1:20 scale models. WARC agreed to treat the model hulls to achieve a friction factor of approximately 0.1 and to prepare a friction test board in a similar fashion. Nippon Kokan Tsu Laboratories (NKK), Tsu City, Japan, who had recently inaugurated an ice towing tank, joined the original facilities in this new phase of the cooperative test program. The results of this second series of tests were reported at the 18th ITTC, October 1987, Kobe, Japan (ITTC 1987).

The results of the test series conducted at CRREL on the smooth model have been reported earlier (Tatinclaux 1984). This report presents the results of the resistance and propulsion tests performed at CRREL with the roughened model and compares the test results obtained with the two models at the facilities involved in the cooperative test program.

SHIP CHARACTERISTICS AND TEST CONDITIONS

Ship characteristics

The Canadian R-class icebreaker was designed to operate continuously in 1-m-thick level ice. The ship has a displacement of approximately 8,000 tons at a midship draft of 6.9 m and is propelled by twin fixed-pitch propellers with a total shaft power of 11,000 kW. The main hull and propeller characteristics at full and model scales are listed in Table 1. A photographs of the model is shown in Figure 1. Three R-class icebreakers are in operation, the CCGS *Radisson*, the CCGS *Franklin* and the CCGS *Des Groseillers*. Full-scale trials have been conducted and reported by Edwards et. al. (1981) for the *Radisson* and by Michailidis and Murdey (1981) for the *Franklin*.

Table 1. Mean characteristics of R-class icebreaker.

		Full scale	*1:20 model*
LWL	Length at waterline	93 m	4.65 m
Lpp	Length between perpendiculars	87.96 m	4.40 m
T	*Level draft*	*6.94 m*	*0.35 m*
B	Maximum waterline beam	19.37 m	0.97 m
	Displacement	7630 m^3	0.95 m^3
CB	Block coefficient	0.611	
C_{max}	Maximum section coefficient	0.918	
C_p	Prismatic coefficient	0.665	
C_w	Waterplane area coefficient	0.799	
Number of propellers		2	
Number of blades per propeller		4	
D	Propeller diameter	4.12 m	0.206 m
Pitch/diameter ratio		0.775	
Expanded area ratio		0.670	
Installed power		11,000 kW	

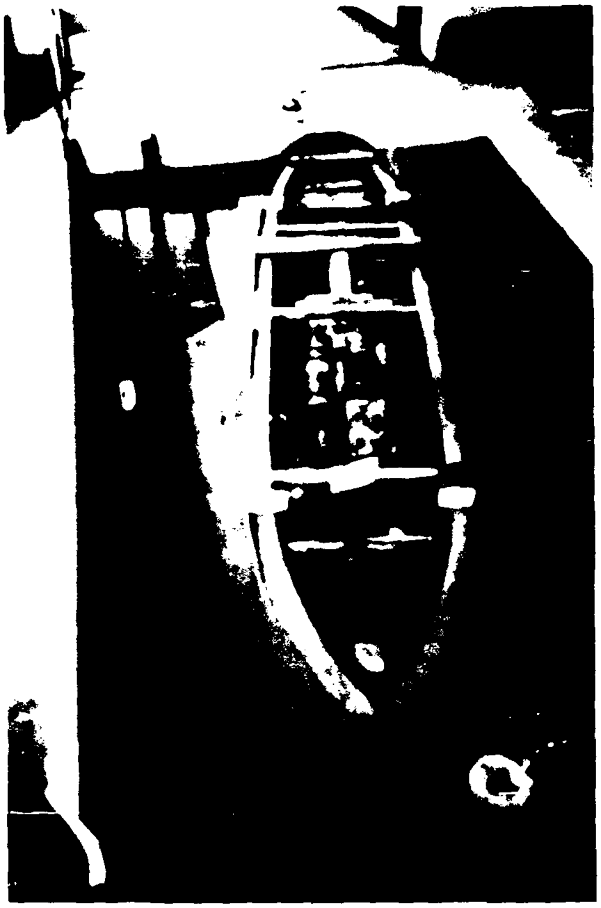

Figure 1. Scale model (1:20) of the R-class icebreaker.

Test conditions

The set of conditions for the resistance and propulsion tests to be performed with the 1:20 scale model, as agreed to by the ITTC Ice Committee members, is given in Table 2.

Table 2. Test conditions.

	Full scale	*Model scale*
Ice thickness, h_i	45 and 70 cm	22.5 and 35 mm
Ice strength, σ_i	400 and 800 kPa	20 and 40 kPa
Ship speed, V	0.5 to 5.0 m/s	0.11 to 1.12 m/s
Range of F_n	0.2 to 2.4	
Range of C_n	60 to 180	

ICE FRICTION FACTOR

As mentioned previously, WARC had treated both the model hull and a special friction plate to achieve an ice friction factor of approximately 0.1. Friction tests were conducted using the plate mounted on a recently built friction table. An ice sample, 13.5 by 13.5 cm in plan dimensions, was inserted into the fixed sample holder that was connected to two load cells. A weight, W, selected to exert the required normal pressure, N, was placed on the sample holder. Both load cells were pre-tensioned and the friction table was set in motion at escribed speed. In most of the friction tests, the table traveled back and forth twice to account for possible minor misalignment of the friction table with respect to the horizontal plane. The average frictional force, T, was measured as the mean of the average forces recorded by the two load cells, $T = (T_1 + T_2)/2$, over a full cycle. The apparent friction coefficient, f_a, was calculated as the ratio

$$f_a = T/(W+W_s) \tag{1}$$

where W_s was the weight of the ice sample and sample holder. The friction test conditions and results are listed in Table 3. All tests were made at the travel speed of approximately 10 cm/s and under wet conditions by pouring a thin film of water over the test plate. No friction tests were made directly on the model hull. The average value of f_a for all the tests performed was found to be 0.086, with a standard deviation of 0.026.

Table 3. Results of ice friction tests.

Normal load W_t (N)	Normal pressure N (kPa)	Tang. force T (N)	Apparent friction factor f_a (x100)
69	3.8	4.9	7.11
69	3.8	5.2	7.51
69	3.8	5.7	8.20
69	3.8	5.7	8.28
69	3.8	4.6	6.57
69	3.8	4.7	6.83
69	3.8	5.0	7.24
69	3.8	5.2	7.44
36.5	2.0	2.7	7.31
36.5	2.0	2.9	7.96
36.5	2.0	3.1	8.40
36.5	2.0	3.2	8.64
16.4	0.9	1.4	8.72
16.4	0.9	1.6	9.81
16.4	0.9	1.7	10.54
16.4	0.9	1.8	10.76
16.4	0.9	1.7	10.16
16.4	0.9	1.8	11.01
16.4	0.9	1.7	10.37
16.4	0.9	1.9	11.34
Averages			
69.3	3.8	5.1	7.4±0.8
36.5	2.0	3.0	8.1±1.3
16.4	0.9	1.7	10.4±3.4

The friction test results are shown in Figure 2a as f_a versus normal pressure, N. It can be seen that the apparent friction factor is decreasing with increasing normal pressure or load. Similar behavior of f_a with N had been observed in a previous study by Forland and Tatinclaux (1985) who attributed this phenomenon to the existence of an adhesion force between the ice sample and the test surface, the origin of which is not yet fully understood. This adhesion force was considered to give rise to an additional tangential stress, τ_o, at the ice/plate interface, the magnitude of which had been found to increase with decreasing ice toughness or ice strength. Thus, the total frictional stress can be expressed as

$$\tau = f_i N + \tau_o \tag{2}$$

where f_i is the actual friction factor. Indeed, when τ is plotted against N as in Figure 2 it is clear that τ is a linear function of N. Linear regression analysis of the test data yielded τ_o = 66 Pa and f_i = 0.071 compared to the average apparent friction factor of 0.086, that is

$$\tau(\text{kPa}) = 0.066 + 0.071\, N(\text{kPa})\,. \tag{2a}$$

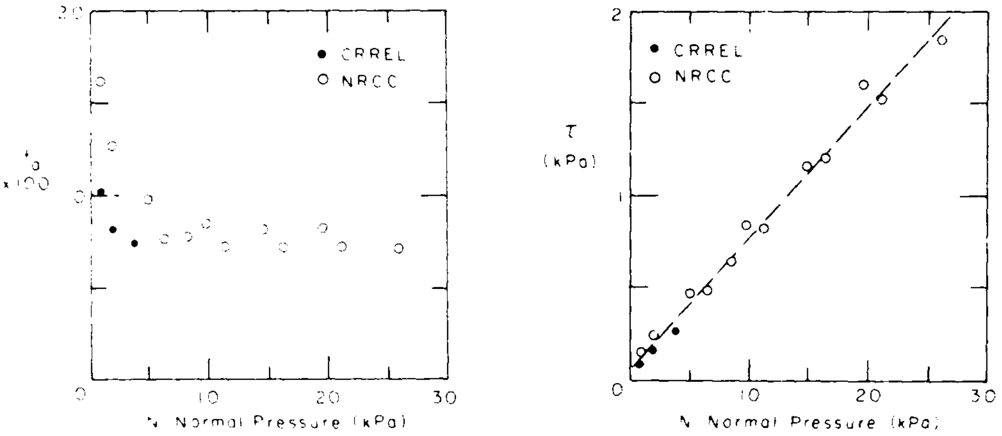

a. Apparent friction factor vs normal pressure.

b. Tangential stress vs normal pressure.

Figure 2. Results of friction tests.

RESISTANCE TESTS WITH ROUGHENED MODEL

Experimental conditions and test results

In the resistance tests, the ship model was connected to the towing carriage by a rigid 7.6-cm (3-in.) diameter towing post that could slide vertically in a linear ball-bearing. The tow post was attached to a force block, mounted on a double-gimbal that was bolted to the bottom of the model. The ship model was thus free to heave, pitch and roll but was totally restrained in surge and sway. It was restricted in yaw by a fork that was attached to the carriage and straddled a vertical rod at the stern of the model. The ship model in the trim tank of the ice towing tank is shown in Figure 1.

For each ice sheet, three tests were made at different velocities, each over a distance of about 10 m or two model lengths. After the first and second tests, the model was backed into the previously broken channel a distance sufficient to allow it to reach steady velocity before it entered the unbroken ice. Before each test series, the ice thickness and flexural strength were measured at several locations along the tank, the latter by the in-situ cantilever beam method. The modulus, or characteristic length of the ice sheet, was not measured. However, for the range of ice strengths used in the study, past experience has shown that the characteristic length of the ice sheet is approximately 10 times its thickness.

The results of the resistance tests are listed in both dimensional and nondimensional form in Table 4. The model resistance in clear water, R_{ow}, was calculated as

$$R_{ow} = 14.53\ V^{1.97} \qquad (3)$$

where R_{ow} is expressed in Newtons and V is the model speed in meters per second. Equation 3 was obtained by regression analysis of the resistance test results by Murdey (1980) with a correlation coefficient $r = 0.997$. Tests at JSRI (ITTC, 1987) have shown negligible effect of the hull roughness on R_{ow}. The net ice resistance was then calculated as $R_i = R_{it} - R_{ow}$. The clear water resistance is usually very small as compared to the ice resistance and well within the range of uncertainty of R_{it}. Only at relatively high speed in thin ice does R_{ow} become a significant component of R_{it}.

Data analysis

Because of the lack of a satisfactory analytical expression for ship resistance in ice, it is customary to fit empirical relationships to the nondimensional data using regression

Table 4. Results of resistance tests in level ice.

	Dimensional data						Nondimensional data			
Test no.	h_i (cm)	σ_i (kPa)	V (m/s)	R_{it} (N)	R_{ow} (N)	R_i (N)	C_n	F_n	$R_{it}/\gamma Bh_i^2$	$R_i/\gamma Bh_i^2$
101	22	28	0.11	23	0.2	22.8	130	0.24	4.99	4.95
102	17	30	0.34	27	1.7	25.3	180	0.83	9.82	9.19
103	20	20	0.57	40	4.8	35.2	102	1.29	10.51	9.25
111	24	24	0.78	67	8.9	58.1	102	1.61	12.22	10.60
112	18	25	1.02	67	15.1	51.9	142	2.43	21.73	16.83
113	23	26	1.23	97	21.8	75.2	115	2.59	19.27	14.93
121	26	21	0.36	43	1.9	41.1	82	0.71	6.68	6.38
122	22	27	0.78	60	8.9	51.1	125	1.68	13.03	11.09
123	24	24	1.26	97	22.9	74.1	102	2.60	17.70	13.52
131	22	20	0.34	36	1.7	34.3	93	0.73	7.82	7.44
132	26	20	0.56	54	4.6	49.4	78	1.11	8.39	7.67
133	24	21	1.00	69	14.5	54.5	89	2.06	12.59	9.94
201	23	40	0.11	29	0.2	28.8	177	0.23	5.76	5.72
202	25	35	0.80	66	9.4	56.6	143	1.62	11.10	9.52
203	24	40	1.24	92	22.2	69.8	170	2.56	16.79	12.74
301	36	27	0.12	48	0.2	47.8	76	0.20	3.89	3.87
302	27	29	0.34	47	1.7	45.3	109	0.66	6.78	6.53
303	32	30	0.57	71	4.8	66.2	96	1.02	7.29	6.79
311	31	25	0.79	76	9.1	66.9	82	1.43	8.31	7.31
312	34	28	1.05	111	16.0	95.0	84	1.82	10.09	8.64
313	29	27	1.24	109	22.2	86.8	95	2.32	13.62	10.85
401	40	45	0.12	77	0.2	76.8	115	0.18	5.06	5.04
402	40	45	0.36	96	1.9	94.1	115	0.57	6.31	6.18
403	40	45	0.52	123	4.0	119.0	115	0.84	8.08	7.81
411	35	60	0.55	90	4.5	85.5	110	1.31	9.44	8.74
412	37	40	0.79	123	9.1	113.9	142	1.68	10.87	9.69
413	36	50	1.00	134	14.5	119.5	175	0.94	7.72	7.34
421	42	43	0.11	94	0.2	93.8	104	0.17	5.60	5.59
422	44	56	0.56	144	4.6	139.4	130	0.85	7.82	7.57
423	42	47	0.99	188	14.2	173.8	114	1.54	11.20	10.35

analysis techniques. The nondimensional ice resistance, $R_* = R_{it}/\gamma Bh_i^2$ or $R_i/\gamma Bh_i^2$, is considered to be primarily a function of Froude number, F_n, based on ice thickness ($F_n = V/\sqrt{gh_i}$) and of the nondimensional ice strength, $C_n = \sigma_i/\gamma h_i$, where B is the beam at the waterline, γ is the specific weight of water and h_i and σ_i are the thickness and flexural strength of ice, respectively. Furthermore, R_* is assumed to be a linear function of C_n and either a first- or a second-degree polynomial in F_n, that is

$$R_* = a\,F_n^2 + b\,F_n + c + d\,C_n \tag{4}$$

or

$$R_* = b\,F_n + c + d\,C_n \tag{5}$$

Regression analyses in accordance with eq 4 or 5 led to the following results. For the total ice resistance, R_{it}

$$R_* = F_n^2 + 2.50\,F_n + 2.68 + 0.0174\,C_n \qquad (r = 0.961) \tag{4a}$$

$$R_* = 5.21\,F_n + 1.16 + 0.0195\,C_n \qquad (r = 0.952) \tag{5a}$$

and for the net ice resistance, R_i

$$R_* = 0.22\,F_n^2 + 2.91\,F_n + 2.74 + 0.0157\,C_n \qquad (r = 0.944) \tag{4b}$$

$$R_* = 3.50\,F_n + 2.41 + 0.0162\,C_n \qquad (r = 0.943). \tag{5b}$$

where r is the correlation coefficient. The correlation coefficients for the two forms of the regression equation being nearly identical indicates that these two forms (eq 4 and 5) are practically indistinguishable. The data are shown graphically in Figures 3a and 3b together with the regression curves, namely eq 4a for the total resistance and eq 5b for the net resistance. In Figures 3c and 3d the calculated values of the total and net resistance, respectively, are plotted against their measured values. It is shown that all measured data fall within ±15% of the calculated values. As in any regression analysis, the values of the coefficients in the regression equations are valid only for the test range of the variables, that is, for the present resistance tests

$$0.17 < F_n < 2.6$$

and

$$60 < C_n < 180.$$

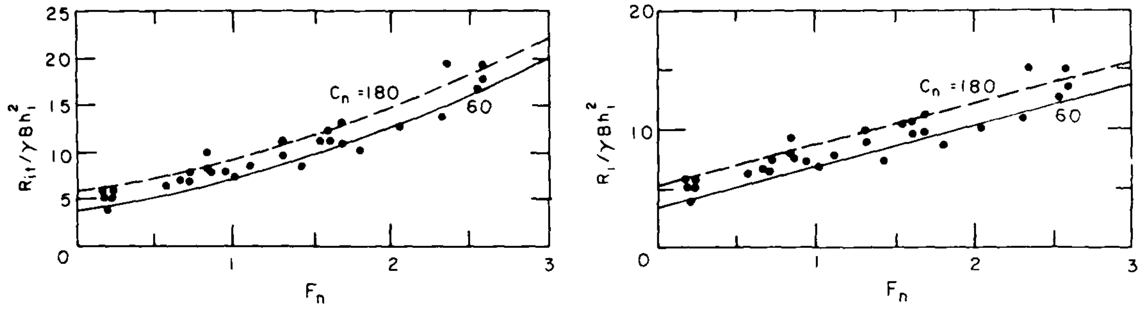

a. Total ice resistance vs Froude number.

b. Net ice resistance vs Froude number.

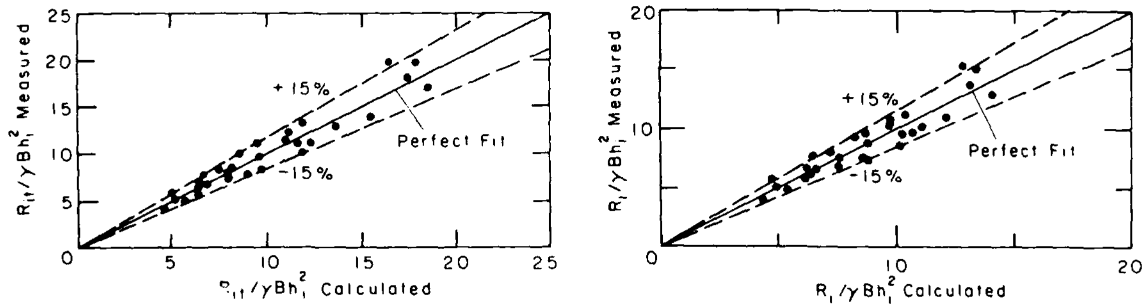

c. Measured vs calculated total resistance.

d. Measured vs calculated net resistance.

Figure 3. Results of resistance tests in level ice.

Comparison with results from smooth model

The results of the resistance tests in ice with the smooth R-class model (ice–hull friction factor of 0.04) have been reported earlier (Tatinclaux 1984). These data were reanalyzed in terms of eq 4 and 5 with the following results. For total resistance in ice, R_{it}

$$R_* = 1.46\,F_n^2 + 0.92\,F_n + 0.07 + 0.0376\,C_n \quad (r = 0.980) \tag{4c}$$

$$R_* = 4.75\,F_n - 1.48 + 0.0381\,C_n \quad (r = 0.964) \tag{5c}$$

and for net ice resistance, R_i

$$R_* = 0.78\,F_n^2 + 1.09\,F_n + 0.19 + 0.0364\,C_n \quad (r = 0.966) \tag{4d}$$

$$R_* = 3.13\,F_n - 0.64 + 0.0367\,C_n \quad (r = 0.958). \tag{5d}$$

The data points for the total resistance of both the smooth and roughened model are plotted in Figure 4a, while those for the net resistance are plotted in Figure 4c. Equations 4a and 4c for the total ice resistance of both models are compared in Figure 4b for the two values of C_n of 60 and 180, the extremes of the test range for C_n. Equations 4b and 4d for the net ice resistance are compared in Figure 4d. At $C_n = 60$, the roughened model exhibits a higher resistance than the smooth model, as expected, but at $C_n = 180$ both models have practically the same resistance. This finding would indicate that for high ice strength, or thin ice, or both, the frictional component is small compared to the breaking component of the total resistance. Increasing hull roughness has then relatively little effect on the resistance.

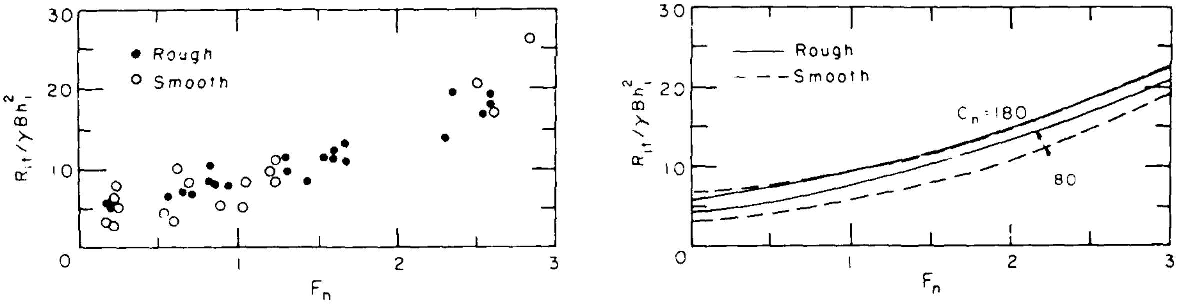

a. Total ice resistance data.

b. Regression function for total resistance.

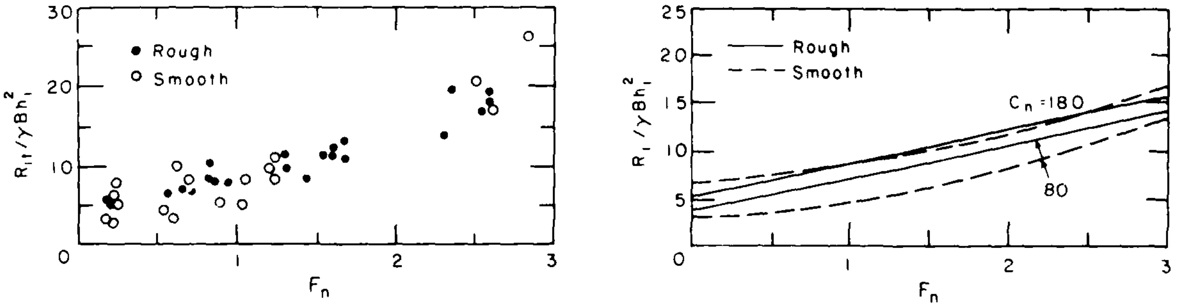

c. Net ice resistance data.

d. Regression function for net resistance.

Figure 4. Comparison between resistance of smooth and roughened models (CRREL data).

PROPULSION TESTS WITH ROUGHENED MODEL

Experimental setup

For the propulsion tests, the R-class model was equipped with two thrust and torque dynamometers, one per propeller shaft, rated at 1100 N in thrust and 11.3 Nm in torque. Both propeller shafts were driven by a single 745-W (1-hp) variable-speed electric dc motor that was equipped with a tachometer servo-mechanism to maintain the rotational speed at the set value. A 1:1.7 gear reducer between the output shaft of the motor and the input shafts of the dynamometers limited the maximum rotational speed of the propeller shafts to about 1000 rpm, the maximum allowable speed for the dynamometers. The shaft speed was measured by a magnetic pickup mounted over a 60-tooth gear fastened to the portside propeller shaft. The frequency of the magnetic pickup was converted to a dc voltage by a frequency-to-voltage converter for digital sampling by the data-acquisition system.

Test procedure

All propulsion tests were made by the captive model technique, whereby the ship model was connected to the towing carriage by the same tow-post–force-block arrangement used in resistance tests. Three tests were made in each ice sheet at the same carriage speed but for three propeller speeds. In each test, the initial values of the thrust and torque from the dynamometers and the initial values from the force block were measured with the propellers running at a very low speed (about 25 rpm) and with the ship model at rest. In this way, the effect of friction between propeller shafts and bushings on the measurements of thrust and, especially, torque was greatly reduced if not eliminated. Also, torque, thrust and, consequently, pull of the propellers are negligible at such low propeller speed. With the ship model still at rest, the propeller speed was increased to the selected value for the particular test and the data acquisition program started.

After approximately 10 seconds under these bollard conditions, the carriage was set in motion at the selected velocity and measurements were taken over about one-third of the tank length. Once the carriage had stopped, data were gathered under bollard conditions for an additional 10 seconds, the propeller speed was then reduced to the initial low value of about 25 rpm and final values were taken for comparison with the initial values, especially values for thrust and torque. The ship model was backed into the broken channel and the procedure repeated for the next test at the same carriage speed and a different propeller speed. The backing distance was such that in the next test the ship model reached steady speed before entering the unbroken ice sheet.

The purpose of the bollard tests at the beginning and the end of each propulsion test was to check the proper functioning of the dynamometers. Throughout the tests, the analog signals from the force block, the thrust and torque outputs of one dynamometer, and the propeller speed counter were monitored on a four-channel chart recorder to ensure visually that all systems were functioning properly.

In each series of three tests per ice sheet, the propeller speed for the first test was selected so that the ship model would be underpropelled, that is the pull would be negative; in the second test, the propeller speed was increased sufficiently to ensure that the model would be overpropelled (positive pull); and in the third test the propeller speed was set at an intermediate value in an attempt to have a pull nearly equal to zero.

In addition to the tests in ice, propulsion tests in clear water were also made for comparison with the test results reported by Murdey (1980). In these tests, the model was towed at constant velocity and the propeller speed was increased at regular intervals along the length of the tank.

The dynamometers and the force block were calibrated by conducting bollard tests in clear water over a wide range of propeller speeds and adjusting the respective calibration coefficients to match the propeller performance reported by Murdey (1980). The bollard thrust and torque for each propeller and the total pull were found to be proportional to the square of the propeller speed, namely, when n_a is expressed in revolutions per second

$$\text{Pull (N)} = 1.175\ n_a^2 \tag{6}$$

$$T_a\text{(N)} = 0.61\ n_a^2 \tag{7}$$

$$Q_a\text{(Nm)} = 0.0199\ n_a^2 \tag{8}$$

which correspond to thrust and torque coefficients of $K_t = 0.339$ and $K_q = 0.0402$, and a thrust deduction factor of $t = 0.04$.

Data acquisition system

Data were acquired on a NEFF 620 system, consisting of a Model 100 signal conditioner and a Model 300 signal processor (analog-to-digital converter), controlled by a HP-9845B desktop computer. Seven data channels were scanned and sampled, namely carriage speed, force block (pull), propeller speed, and thrust and torque of both propellers. The sampling rate, S (in milliseconds), of the analog signals was selected so that a minimum of 32 samples were taken per propeller revolution (8 samples per propeller blade), that is

$$2 < S(\text{ms}) < 1000/(32n_a).$$

The data in digitized form were stored on floppy disks for subsequent analysis. An example of the data signals is shown in Figure 5.

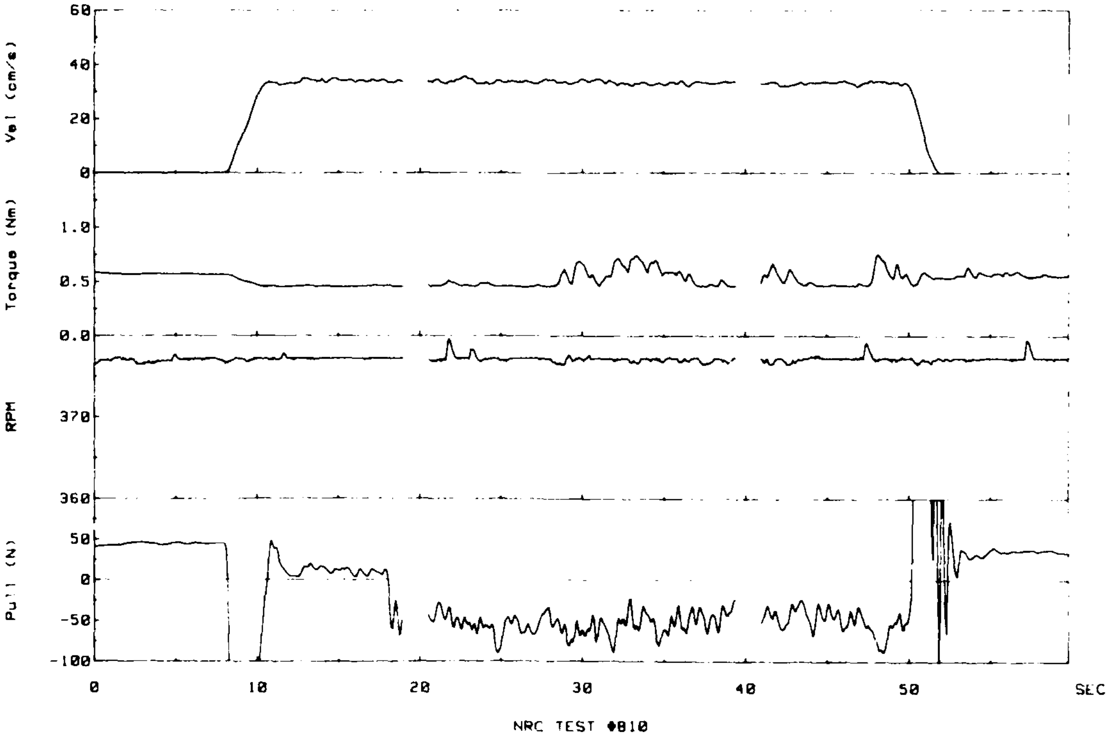

a. Carriage velocity, starboard torque, propeller speed and pull.

Figure 5. Example of data signals for test no. 810 (h_i = 3.5 mm; σ_i = 20 kPa, V = 0.35 m/s; n_a = 377 rpm).

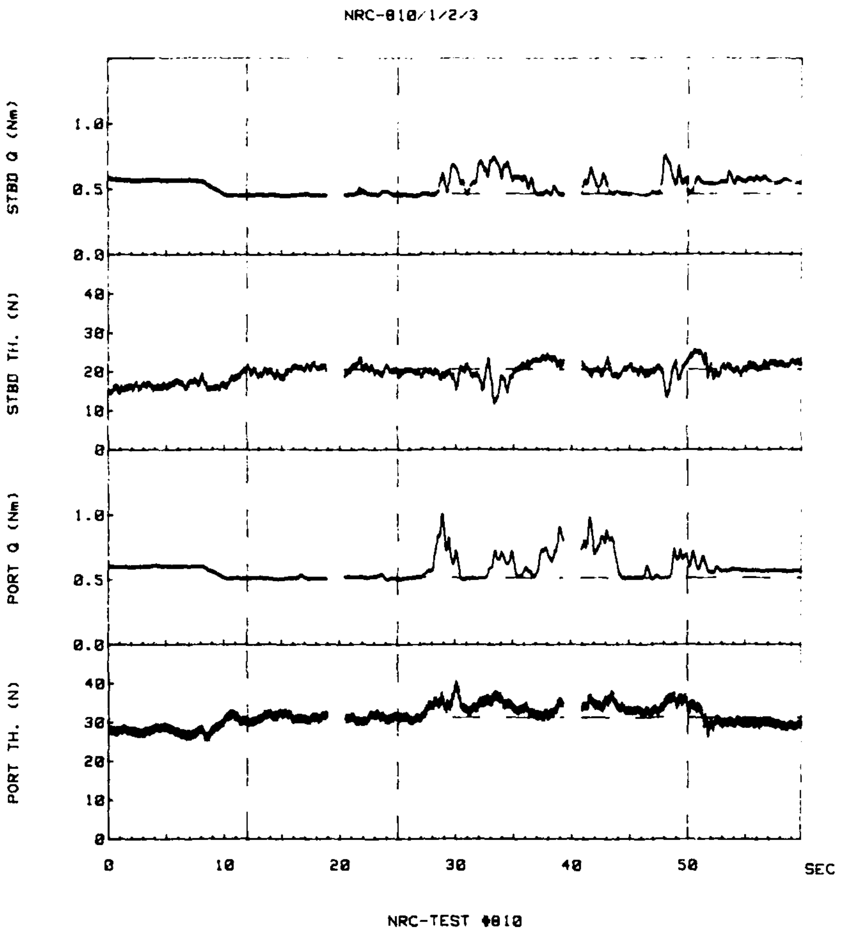

b. Thrust and torque on both propellers.

Figure 5 (cont'd).

Data presentation and analysis

Data presentation

For each test, the data were averaged over the period of uniform carriage velocity. The test data in dimensional form are listed in Table 5 and in nondimensional form in Table 6, where J_a is the appparent advance coefficient, K_t the thrust coefficient and K_q the torque coefficient, defined as

$$J_a = V/n_a D \tag{9}$$

$$K_t = T_a/(2\rho\, n_a^2 D^4) \tag{10}$$

$$K_q = Q_a/(2\, \rho n_a^2 D^5) \tag{11}$$

where ρ is water density and D propeller diameter.

Self-propulsion points

The results of the three propulsion tests carried out at a given carriage velocity in one ice sheet were interpolated to the point of zero pull to obtain the self-propulsion point for the

Table 5. Results of propulsion tests with roughened R-class model.

Test no.	h_i (mm)	σ_f (kPa)	V (m/s)	n_a (rpm)	Pull (N)	Port T_a (N)	Port Q_a (Nm)	Starboard T_a (N)	Starboard Q_a (Nm)
a. Tests in level ice									
511	38	45	0.34	398	–72	21.7	0.78	21.5	0.87
512				600	–11	55.2	1.42	53.6	1.47
513				653	21	64.9	1.64	64.6	1.64
552	31	45	0.52	400	–47	17.9	0.75	17.9	0.61
551				500	NA	32.9	1.05	27.8	1.51
553				702	41	67.2	1.93	68.3	1.98
521	37	32	0.74	599	–47	38.1	1.97	42.9	1.19
522				708	–23	55.4	2.34	59.1	2.16
523				757	10	69.9	2.34	69.9	2.37
543	25	25	0.52	393	–15	18.0	0.62	17.9	0.62
541				497	0	32.3	0.98	30.7	1.04
542				602	37	49.8	1.37	52.1	1.34
531	26	26	0.76	498	–35	22.9	1.00	21.8	1.21
532			0.75	600	–5	35.6	1.53	38.9	1.56
533			0.74	625	8	45.3	1.52	45.6	1.56
561	22	33	1.24	707	–27	39.5	1.74	41.5	1.68
562			1.20	760	–10	54.1	2.32	54.0	2.39
653			1.20	812	6	64.1	2.47	66.5	2.45
b. Tests in clear water									
911			0.34	541	78	43.0	1.01	42.6	1.02
912				482	60	33.7	0.81	34.1	0.82
913				410	42	25.4	0.56	23.7	0.55
914				343	25	14.9	0.36	15.8	0.37
915				275	16	9.1	0.21	9.5	0.23
916				211	5	4.7	0.12	4.8	0.09
921			0.52	541	68	40.8	1.00	37.1	0.93
922				483	50	30.1	0.77	28.9	0.71
923				418	39	21.3	0.55	20.9	0.51
924				338	21	12.6	0.31	12.6	0.30
925				262	8	6.1	0.16	6.6	0.17
931			0.74	707	110	64.5	1.67	61.2	1.57
932				604	69	45.4	1.19	43.9	1.11
933				515	43	29.5	0.81	29.4	0.75
934				410	20	15.0	0.43	16.1	0.39
935				325	6	6.5	0.22	7.6	0.21
941			1.20	749	59	52.2	1.52	55.0	1.55
942				658	39	39.4	1.13	40.4	1.14
943				555	13	24.0	0.63	25.0	0.68

Table 6. Nondimensional form of propulsion test results.

Test no.	F_n	C_n	J_a	K_t	K_q
		a. Tests in level ice			
511	0.56	121	0.25	0.274	0.0505
512			0.17	0.302	0.0390
513			0.15	0.304	0.0373
552	0.94	148	0.38	0.224	0.0412
553			0.30	0.243	0.0497
551			0.22	0.275	0.0385
521	1.23	88	0.36	0.226	0.0427
522			0.30	0.228	0.0436
523			0.28	0.244	0.0399
543	1.05	102	0.39	0.232	0.0390
541			0.30	0.255	0.0397
542			0.25	0.281	0.0363
531	1.50	102	0.44	0.180	0.0432
532	1.49		0.36	0.207	0.0416
533	1.47		0.34	0.233	0.0383
561	2.67	153	0.51	0.162	0.0332
562	2.58		0.46	0.187	0.0396
563	2.58		0.43	0.198	0.0362
		b. Tests in clear water			
911			0.18	0.292	0.0337
912			0.21	0.292	0.0340
913			0.24	0.292	0.0320
914			0.29	0.261	0.0301
915			0.36	0.246	0.0282
916			0.47	0.213	0.0229
921			0.28	0.266	0.0320
922			0.32	0.253	0.0308
923			0.36	0.241	0.0294
924			0.45	0.221	0.0259
925			0.58	0.185	0.0233
931			0.31	0.251	0.0315
932			0.36	0.245	0.0306
933			0.42	0.222	0.0285
934			0.53	0.185	0.0237
935			0.66	0.133	0.0198
941			0.47	0.191	0.0266
942			0.53	0.184	0.0254
943			0.63	0.159	0.0206

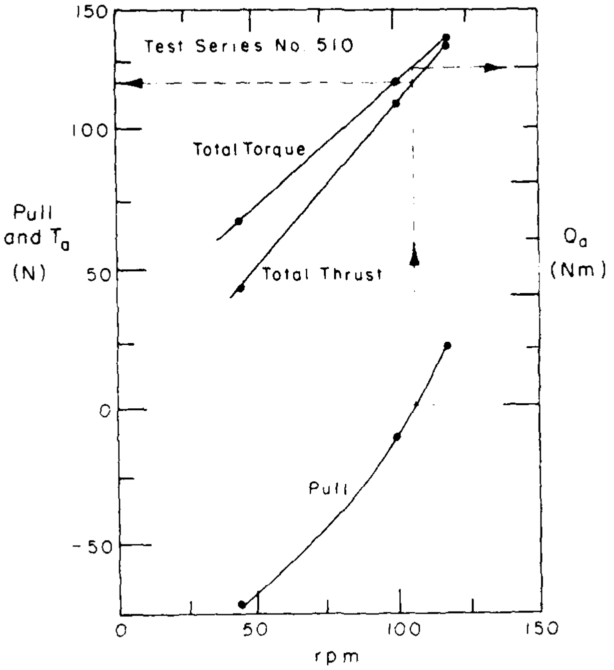

Figure 6. Example of determination of self-propulsion point by interpolation of propulsion test results (test series 510).

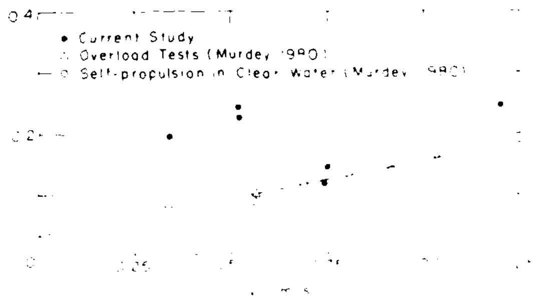

Figure 7. Thrust deduction factors from several studies.

Table 7. Self-propulsion points in ice of roughened R-class model.

Test series	h_i *(mm)*	σ_i *(kPa)*	V *(m/s)*	R_{it} *(N)*	n_a *(rpm)*	*Total* T_a*(N)*	*Total* Q_a*(Nm)*	J_a	K_t	$10K_q$	t
510	38	45	0.34	93	620	116	3.01	0.16	0.304	0.382	0.20
550	31	45	0.52	84	643	111	3.43	0.24	0.269	0.404	0.24
520	37	32	0.74	117	744	133	4.71	0.29	0.240	0.413	0.12
540	25	25	0.52	50	497	65	2.02	0.30	0.262	0.397	0.23
530	26	26	0.75	70	610	82	3.05	0.36	0.210	0.395	0.15
560	22	33	1.20	92	786	122	4.78	0.45	0.197	0.375	0.25

Note: Total resistance $R_{it} = R_i + R_{ow}$, with R_i given by eq 4b and R_{ow} by eq 3.

corresponding ice thickness, ice strength and ship speed. An example of this interpolation procedure is shown in Figure 6. The self-propulsion points thus obtained are given in Table 7, where $R_{it} = R_i + R_{ow}$; R_i was calculated according to eq 4b and the thrust deduction factor was defined by

$$t = 1 - R_{it}/T_a. \tag{12}$$

The accuracy of the thrust deduction factor, *t*, depends on the accuracy of the resistance estimate and of the thrust measurements. For given ice conditions of thickness and flexural strength, ship resistance in level ice, in contrast with that in ice-free water, can usually be estimated at best within ±10% of its actual value. Therefore, even if the propeller thrusts are accurately measured, significant uncertainties remain in the values of *t* calculated from the results of independent resistance and propulsion tests. Figure 7 presents the values of *t* at the self-propulsion points as determined in the present study. Also shown in Figure 7 are the values of *t* evaluated from the results of overload tests in ice-free water (Murdey 1980) for the conditions of model speed and propeller speed corresponding to the self-propulsion points in ice, and the values of *t* obtained by Murdey (1980) at the self-propulsion points in clear water. As can be seen from Figure 7, the values of *t* in level ice are scattered about those in ice-free water.

Until a better method to evaluate the thrust deduction factor in ice is available, it is recommended that the values obtained under clear water conditions be used. In the present case, they can be expressed by

$$t = 0.04 + 0.12\,V \tag{13}$$

which is valid for $V < 1.20$ m/s, the maximum speed in the present test series. If it is assumed that the thrust deduction is the same at full scale and at model scale for corresponding ship and model speeds, then the expression for *t* at full scale is

$$t = 0.04 + 0.027\,V. \tag{14}$$

Equation 14 is valid for $V < 5.37$ m/s at full scale.

The results of propulsion tests with the smooth model had led to the conclusion that the thrust deduction factor, *t*, in level ice was constant, independent of velocity and equal to about 0.20. Because of doubts about the proper functioning of the thrust dynamometers during this previous study, as explained below, eq 13 and 14 are assumed to apply also to the results with the smooth model in the following analyses and extrapolation to full-scale conditions.

Propeller coefficients

The thrust and torque coefficients, K_t and K_q, for all propulsion tests both in level ice and in ice-free water are plotted versus J_a on Figure 8, where the values of K_t and K_q obtained with the smooth model are also shown. It can be seen that the thrust coefficient for the rougher model in level ice is only slightly smaller than that in ice-free water. K_t for the smooth model from the previous study was generally higher than K_t for both the rougher model and the ice-free conditions. This latter observation would indicate inaccuracies in or malfunction of the thrust dynamometer during the previous study. Therefore, in the following analyses and full-scale extrapolations, the thrust coefficients obtained from the present propulsion tests were assumed valid for both the rough and smooth model. On the other hand, the values of K_q obtained in both studies from propulsion tests in level ice are comparable and consistently greater than those for the ice-free conditions. The changes in K_t and K_q between level ice and ice-free conditions are attributed to ingestion of ice floes by the propellers. The resulting impacts of the propeller blades on ice floes increase the torque on the propellers and decrease the thrust delivered by the propellers. The experimental data were analyzed using linear regression and forcing the regression curves to pass through the respective values of K_t and K_q at bollard. For ice-free conditions, the resulting equations were

$$K_t = 0.339 - 0.303\,J_a \quad (r = 0.986) \tag{15}$$

and

$$K_q = 0.0402 - 0.0308\,J_a \quad (r = 0.969). \tag{16}$$

For the case of level ice conditions, the equations were

$$K_t = 0.339 - 0.318\,J_a \quad (r = 0.972) \tag{17}$$

and

$$K_q = 0.0402 - 0.0066\,J_a \quad (r = 0.38). \tag{18}$$

These equations are shown in Figure 8.

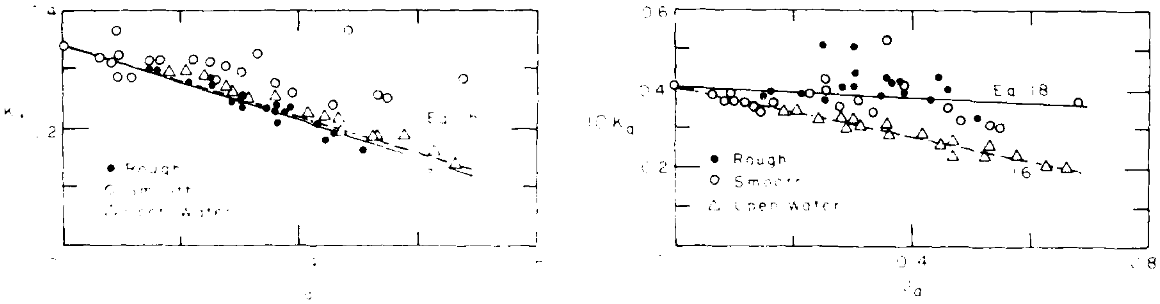

a. Thrust coefficient.

b. Torque coefficient.

Figure 8. Propulsion coefficients vs apparent advance coefficient.

FULL-SCALE PERFORMANCE PREDICTIONS AND COMPARISON WITH EXISTING DATA

Performance predictions

Equations 5b, 4d and 14 to 18 are the basis for predicting full-scale performance from the model test results. For the hull and propeller characteristics of the R-class icebreaker, these equations become

$$R_i\ (\mathrm{kN}) = 212.3\ V h_i^{1.5} + 458.0 h_i^2 + 0.314 \sigma_i h_i \quad \text{(rough)} \tag{19a}$$

$$R_i\ (\mathrm{kN}) = 15.1\ V^2 h_i + 66.1\ V h_i^{1.5} + 36.1 h_i^2 + 0.705 \sigma_i h_i \quad \text{(smooth)} \tag{19b}$$

$$R_{it} (\mathrm{kN}) = R_i + R_{ow} \tag{20}$$

$$T_a\ (\mathrm{kN}) = R_{it} / (0.96 - 0.027\ V) \tag{21}$$

$$T_a\ (\mathrm{kN}) = 195\ n_a^2 - 44.5\ V n_a \qquad \text{(level ice)} \tag{22a}$$

$$T_a\ (\mathrm{kN}) = 195\ n_a^2 - 42.4\ V n_a \qquad \text{(clear water)} \tag{22b}$$

$$Q_a (\mathrm{kNm}) = 95.4\ n_a^2 - 3.80\ V n_a \qquad \text{(level ice)} \tag{23a}$$

$$Q_a (\mathrm{kNm}) = 95.4\ n_a^2 - 17.8\ V n_a \qquad \text{(clear water)} \tag{23b}$$

$$PD\ (\mathrm{kW}) = 2\pi\ n_a Q_a \tag{24}$$

In eq 20, R_{ow} is the full-scale resistance in ice-free water. This resistance was predicted from model test experiments by Murdey (1980). For the purpose of comparing the predicted ship performance in level ice with existing full-scale trial data, Murdey's results were expressed in the following form

$$R_{ow} (\mathrm{kN}) = 4.41\ V + 2.56\ V^2 + 0.155\ V^3 \qquad (V < 6\ \mathrm{m/s}) \tag{25a}$$

$$R_{ow}\ (\mathrm{kN}) = 152 + 54\ (V - 6) + 14.2\ (V - 6)^3 \qquad (V > 6\ \mathrm{m/s}) \tag{25b}$$

In eq 19–25, h_i is in meters, V in meters per second, σ_i in kilopascals, and n_a in s^{-1} (revolutions per second). It should be reiterated that these equations are strictly valid within the experimental range 0.17–2.6 for the Froude number, F_n, and within the range 60–180 for the dimensionless ice strength, C_n.

Predicted total resistance, total thrust and shaft power for the conditions h_i = 0.45 and 0.70 m and σ_i = 450 and 600 kPa are presented in Table 8 for both models and plotted in Figure 9 for the smooth model and in Figure 10 for the rough model. Conversely, given shaft power and ice strength, eq 19–25 can be used to predict the speed at which the vessel will break level ice of given thickness. Such performance predictions of V vs h_i at full power of 11,000 kW for ice strength of 450 kPa are listed, with corresponding ice resistance and total thrust, in Table 9a where the values of K_t and K_q from propulsion tests in level ice were used, and in Table 9b where those from tests in clear water were used. The tables contain predictions based on the resistance equations derived from the resistance test results with the smooth model and the roughened model. These predicted performances are shown as maximum velocity at full power versus ice thickness in Figure 11a for the smooth model and in Figure 11b for the roughened model.

Table 8. Predicted performance of both models for given ice conditions (K_t and K_q from model tests in ice).

Ice conditions	V(*kn*)	*Smooth model*			*Rough model*		
		R_{it}(*MN*)	T_a(*MN*)	PD(*MW*)	R_{it}(*MN*)	T_a(*MN*)	PD(*MW*)
	3	0.21	0.23	1.18	0.27	0.29	1.61
	4	0.24	0.27	1.64	0.31	0.34	2.23
h_i=0.45 m	5	0.28	0.31	2.25	0.35	0.40	3.00
σ_i=450 kPa	6	0.32	0.36	3.04	0.40	0.45	3.93
	7	0.37	0.42	4.05	0.44	0.51	5.04
	8	0.42	0.49	5.31	0.49	0.58	6.36
	3	0.34	0.37	2.18	0.53	0.58	3.99
	4	0.39	0.43	2.95	0.60	0.66	5.27
h_i=0.70 m	5	0.44	0.49	3.95	0.67	0.76	6.81
σ_i=450 kPa	6	0.50	0.57	5.22	0.75	0.86	8.61
	7	0.57	0.66	6.81	0.83	0.96	10.70
	8	0.65	0.77	8.78	0.91	1.07	13.12
	3	0.26	0.28	1.53	0.29	0.32	1.78
	4	0.29	0.32	2.04	0.33	0.37	2.43
h_i=0.45 m	5	0.32	0.36	2.71	0.37	0.42	3.22
σ_i=600 kPa	6	0.37	0.42	3.57	0.42	0.48	4.18
	7	0.41	0.48	4.64	0.46	0.54	5.32
	8	0.47	0.55	5.99	0.51	0.61	6.67
	3	0.41	0.45	2.85	0.56	0.61	4.33
	4	0.46	0.51	3.71	0.63	0.70	5.66
h_i=0.70 m	5	0.51	0.58	4.81	0.71	0.79	7.24
σ_i=600 kPa	6	0.58	0.66	6.19	0.78	0.89	9.09
	7	0.65	0.75	7.89	0.86	1.00	11.24
	8	0.72	0.85	9.98	0.94	1.11	13.71

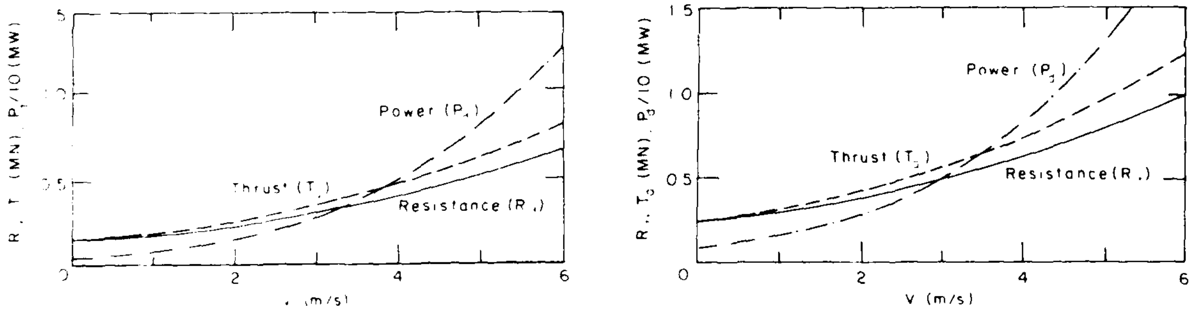

a. h_i = *0.45 m;* σ_i = *450 kPa.*

b. h_i = *0.70 m;* σ_i = *450 kPa.*

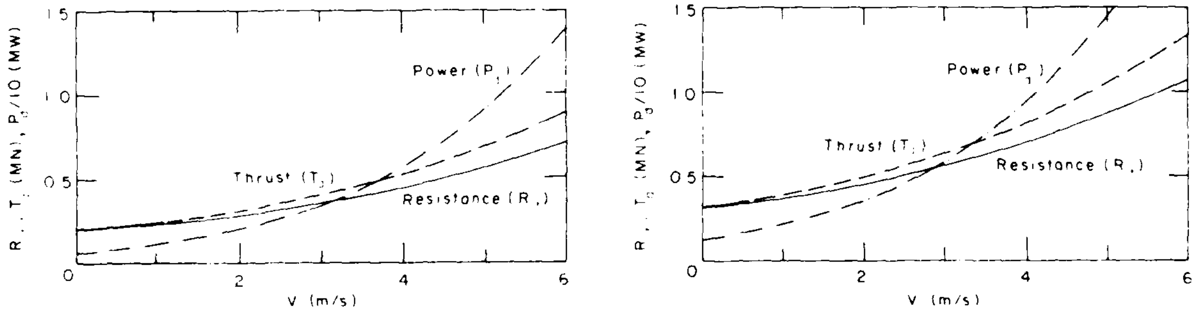

c. h_i = *0.45 m;* σ_i = *600 kPa.*

d. h_i = *0.70 m;* σ_i = *600 kPa.*

Figure 9. Predicted performance in level ice from test results with smooth model (K_t *and* K_q *from tests in level ice).*

Table 9. Predicted performance in level ice at full power.

σ_i (kPa)	h_i (m)	*Smooth model* V (kn)	*Smooth model* R_{it} (MN)	*Smooth model* T_a (MN)	*Rough model* V (kn)	*Rough model* R_{it} (MN)	*Rough model* T_a (MN)
		a. K_t and K_q from model tests in ice.					
450	0.20	13.7	0.48	0.60	14.4	0.45	0.56
	0.30	12.6	0.54	0.67	13.0	0.51	0.64
	0.40	11.4	0.59	0.73	11.4	0.59	0.74
	0.50	10.5	0.64	0.78	9.9	0.68	0.82
	0.60	9.7	0.69	0.83	8.4	0.76	0.90
	0.70	8.9	0.73	0.87	7.1	0.84	0.97
	0.80	8.2	0.77	0.91	5.9	0.91	1.04
	0.90	7.6	0.81	0.95	4.9	0.98	1.10
	1.00	7.0	0.84	0.98	3.9	1.04	1.15
600	0.20	13.5	0.49	0.61	14.3	0.46	0.57
	0.30	12.3	0.55	0.69	12.9	0.52	0.65
	0.40	11.1	0.61	0.75	11.2	0.60	0.74
	0.50	10.1	0.66	0.81	9.7	0.69	0.83
	0.60	9.2	0.71	0.86	8.2	0.77	0.91
	0.70	8.4	0.76	0.90	6.9	0.85	0.99
	0.80	7.7	0.80	0.94	5.7	0.93	1.05
	0.90	7.0	0.84	0.98	4.6	1.00	1.11
	1.00	6.4	0.88	1.01	3.6	1.06	1.17
		b. K_t and K_q from model tests in clear water.					
450	0.20	16.0	0.75	0.94	16.6	0.74	0.92
	0.30	15.0	0.77	0.97	15.7	0.76	0.94
	0.40	13.9	0.80	0.99	14.3	0.79	0.98
	0.50	12.7	0.82	1.03	12.3	0.83	1.04
	0.60	11.5	0.85	1.06	10.3	0.89	1.09
	0.70	10.6	0.88	1.09	8.6	0.96	1.14
	0.80	9.7	0.92	1.11	7.1	1.02	1.18
	0.90	8.9	0.95	1.13	5.7	1.07	1.22
	1.00	8.2	0.97	1.15	4.5	1.12	1.25
600	0.20	15.9	0.75	0.94	16.6	0.74	0.92
	0.30	14.8	0.77	0.97	15.6	0.76	0.95
	0.40	13.6	0.80	1.00	14.2	0.79	0.99
	0.50	12.2	0.83	1.04	12.1	0.84	1.05
	0.60	11.0	0.87	1.08	10.1	0.90	1.10
	0.70	10.0	0.91	1.10	8.4	0.97	1.15
	0.80	9.1	0.94	1.13	6.8	1.03	1.19
	0.90	8.3	0.97	1.15	5.4	1.08	1.22
	1.00	7.5	1.00	1.17	4.2	1.13	1.26

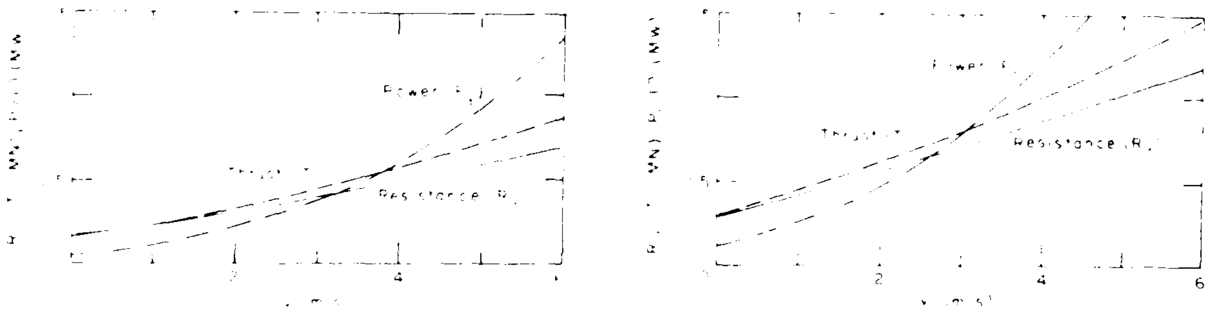

a. h_i = 0.45 m; σ_i = 450 kPa.

b. h_i = 0.70 m; σ_i = 450 kPa.

Figure 10. Predicted performance in level ice from test results with roughened model (K_t and K_q from tests in level ice).

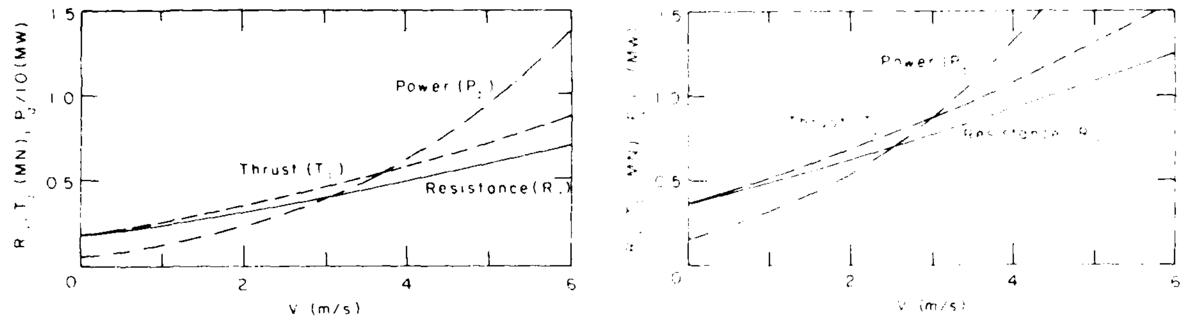

c. $h_i = 0.45$ m; $\sigma_i = 600$ kPa.

d. $h_i = 0.70$ m; $\sigma_i = 600$ kPa.

Figure 10 (cont'd).

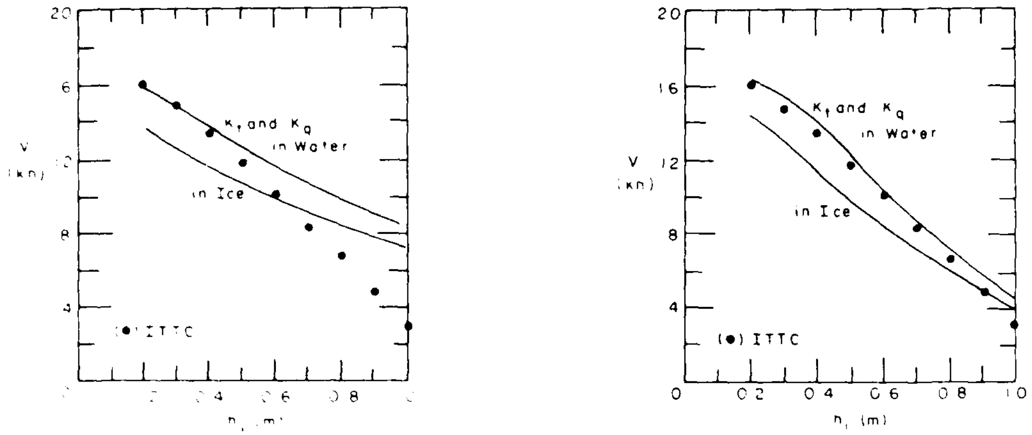

a. Smooth model.

b. Roughened model.

Figure 11. Predicted performance: V vs h_i at constant power (with $\sigma_i = 450$ kPa, t from clear water tests and K_t and K_q from tests in level ice and in clear water).

Comparison between predictions and measurements

In its report to the 18th International Towing Tank Conference (ITTC 1987), the Ice Committee presented a reanalysis of available full-scale data from trials with the CCGS *Radisson* (Edwards et al. 1981) and the CCGS *Franklin* (Michailidis and Murdey 1981). These adjusted full-scale data, corresponding to ice strength of either 400 or 480 kPa, are given in Table 10. In addition, the particular set of full-scale data by Michailidis and Murdey (1981) are listed in Table 11 as they appear to the writers as being the best available set of field data with the R-class icebreaker. Both sets of data are plotted in Figures 11a and 11b for comparison with the above ship performance predictions.

From these figures it can be seen that the performance predictions based on the roughened model resistance and the values of K_t and K_q in clear water are in very good agreement with the full-scale data, especially for ice thicknesses less than 0.8 m. This observation must be interpreted as a strong indication that effect on propeller performance of ice ingestion into the propeller disks is far greater at model scale than at full scale. This exaggerated ice effect at model scale can be caused by more, and relatively larger, ice floes being ingested by the propellers than at full scale because of incorrect modeling of ice properties, such as density, bulk modulus and fracture toughness.

Table 10. Full-scale data for R-class performance in level ice (ITTC 1987).(Full-scale ice flexural strength was 407 or 480 kPa.)

a. Speed in level ice at full power (11,000 kW).

h_i (*m*)	V(*kn*)
0.2	15.9
0.3	14.7
0.4	13.3
0.5	11.7
0.6	10.0
0.7	8.2
0.8	6.6
0.9	4.7
1.0	2.9

b. *Total resistance, thrust and power in 0.7-m level ice.*

V (*kn*)	R_{it} (*MN*)	T (*MN*)	PD (*MW*)
3	0.50	0.54	3.43
4	0.54	0.58	4.00
5	0.59	0.65	4.93
6	0.65	0.74	6.21
7	0.74	0.85	7.75
8	0.85	0.97	9.36

Table 11. Full-scale trial data (after Michailidis and Murdey 1981).

V(*kn*)	h_i(*m*)	h_s(*M*)	σ(*kPa*)	*rpm*	P(*kW*)	T_d(*kN*)
			Port propeller			
2.18	0.704	0.08	510	115.7	1840	289.0
4.64	0.620	0.13	480	126.3	2320	318.8
5.38	0.674	0.08	460	132.6	2560	348.7
4.05	0.676	0.15	NA	142.6	3700	413.5
7.06	0.650	0.11	NA	155.7	4180	443.4
8.23	0.666	0.12	NA	170.3	5420	528.1
7.64	0.613	0.09	NA	162.4	4610	478.3
			Starboard propeller			
2.18	0.704	0.08	510	122.0	2020	289.0
4.64	0.620	0.13	480	127.0	2190	328.8
5.38	0.674	0.08	460	133.9	2950	358.7
4.05	0.676	0.15	NA	146.4	3750	413.5
7.06	0.650	0.11	NA	154.7	3840	473.3
8.23	0.666	0.12	NA	173.8	5480	523.1
7.64	0.613	0.09	NA	164.6	4580	478.3

COMPARISON WITH RESULTS FROM OTHER FACILITIES

As mentioned in the *Introduction*, this series of ship model tests was part of an international cooperative effort under the aegis of the ITTC. The results of the resistance and propulsion tests made with the smooth model by the various participating organizations were presented at the 1984 ITTC in Göteborg, Sweden (ITTC 84). The results of the resistance tests with the roughened model were reported by the Ice Committee to the 18th ITTC in Kobe, Japan (ITTC 87). The results of the propulsion tests with the latter model, which have not yet been completed by all facilities, are to be presented at the 19th ITTC in 1990 in Madrid, Spain. The results of the resistance and propulsion tests on both the smooth and roughened 1:20 scale R-class model by the various facilities are listed in Appendix A.

Data on resistance and propulsion performance from ship model tests in ice are analyzed by using standard linear, multilinear or nonlinear regression analysis methods. Since there exists no satisfactory analytical formulation of the interaction between ship and ice to suggest the form of the regression equation, the choice of this equation is arbitrary and left to the individual researcher. Based on their experience, the writers have assumed that the selected dependent variable (e.g., nondimensional resistance, thrust or torque coefficient) could be expressed as a first or second degree polynomial of the independent variables (e.g., Froude number, nondimensional ice strength or advance coefficient). For any regression analysis of experimental data to yield reasonably reliable results, the data set should be large enough and more than one test should have been made for the same experimental conditions to check the repeatablity of the data. Finally, when comparing several data sets, the range of the independent variables should be nearly the same from one data set to another.

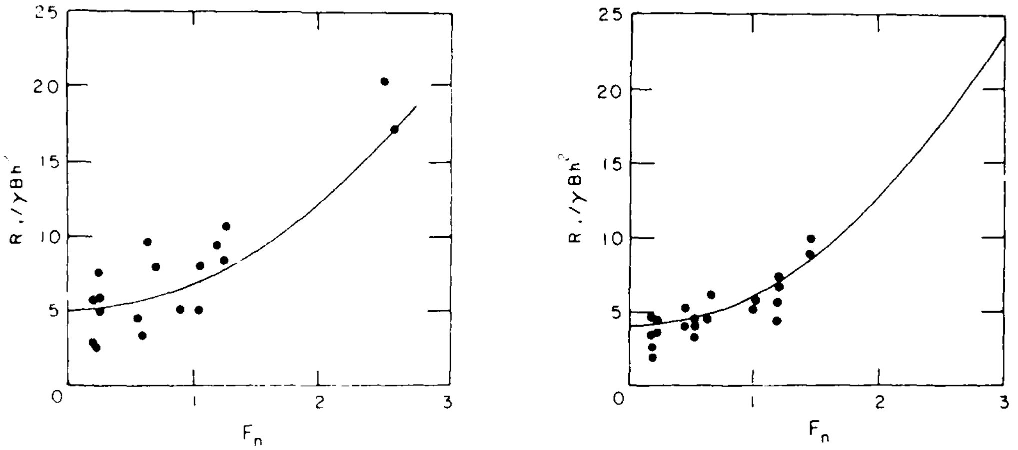

a. CRREL.

b. HSVA.

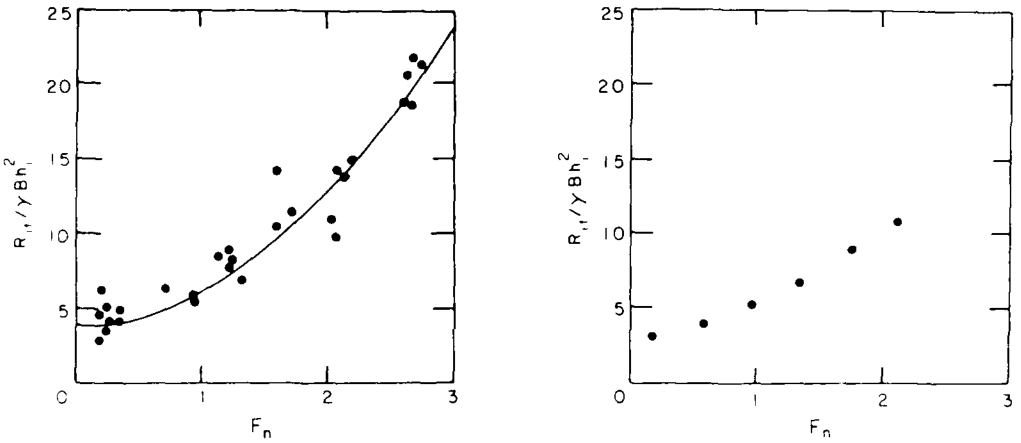

c. JSRI

d. NKK

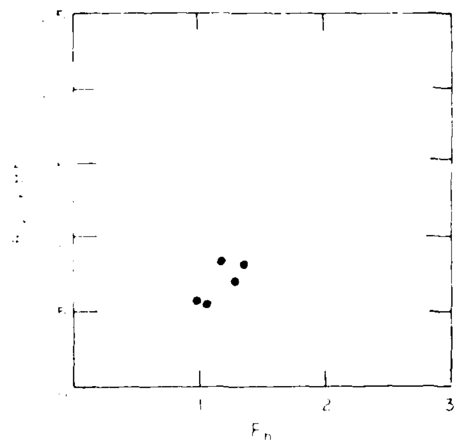

e. WARC

Figure 12. Resistance test results at participating facilities with smooth R-class model.

Table 12. Range of resistance test conditions with smooth model

Facility	*No. of Tests*	h_i*(mm)*	σ_i*(kPa)*	V*(m/s)*	F_n	C_n
		Range of test conditions				
CRREL	20	20–40	25–55	0.11–1.31	0.19–2.85	64–261
HSVA	25	22–51	18–43	0.10–0.71	0.16–1.45	50–182
JSRI	33	10–37	27–65	0.11–1.23	0.19–3.95	100–570
NKK	6	35–36	39–44	0.11–1.24	0.19–2.12	114–125
WARC	7	19–36	19–32	0.58–0.59	0.98–1.34	74–107

Note: Ice thicknesses were rounded to the nearest millimeter, and ice strengths to the nearest kilopascal.

Tests with smooth model

Resistance tests

Five facilities, CRREL, HSVA, JSRI, NKK and WARC, conducted resistance tests in level ice with the smooth 1:20 scale R-class model. The range of test conditions at these various facilities is listed in Table 12, and the test data are plotted in Figure 12.

Note that both NKK and WARC conducted only a very limited number of tests. Furthermore, all NKK tests were made at practically constant ice thickness and ice strength (ice strength can usually be measured with no better than a 10% accuracy), and velocity was the only independent variable. On the contrary, all WARC tests were made at a single velocity, and at only two ice thicknesses and two ice strengths; therefore, the corresponding data are insufficient for a reliable regression analysis involving more than one independent variable.

Statistical analysis of all test data indicated that the model total ice resistance, R_{it}, was mainly influenced by model speed, V, and ice thickness, h_i, and only marginally affected by ice strength, σ_i. Consequently, the nondimensional ice resistance, $R_* = R_{it}/\gamma B h_i^2$, is primarily a function of the Froude number, $F_n = V/\sqrt{g h_i}$, and varies only weakly with $C_n = \sigma_i/\gamma h_i$, as is evident from Figure 13a. Table 13 shows the distribution of the tests with the smooth R-class model among various Froude number ranges.

Only four tests were conducted at F_n greater than 2.75, one by CRREL and three by JSRI. As can be seen from Table A1 and Figure 13a, each of these four tests was made at a distinct value of F_n; that is, the repeatability of the test results at very high F_n cannot be assured. Since such isolated points at the extreme end of the range of an independent variable may significantly bias the results of a regression analysis, these points were not taken into account in the analyses presented below.

Two forms of the regression equation relating the nondimensional resistance in level ice, R_*, to the independent variables, F_n and C_n, were considered. Form I assumed that R_* was a second degree polynomial in F_n and linear in C_n. The corresponding coefficients are listed in Table 14a for the total resistance and for the net resistance. Because the coefficient of F_n in form I of the regression equation is relatively small and has a wide range of uncertainty, as indicated by its 90% confidence interval, a second form (form II) of the regression equation was then considered where R_* is only a linear function of F_n^2 and C_n, i.e., $R_* = A + B \cdot F_n^2 +$

Table 13. Resistance test distribution with respect to Froude number (smooth model).

Froude no. range	*CRREL*	*HSVA*	*JSRI*	*NKK*	*WARC*	*Total*
	Facility					
0–0.25	6	9	7	1	0	23
0.25–0.50	1	2	2	0	0	5
0.50–0.75	4	6	1	1	0	12
0.75–1.25	5	6	6	1	5	23
1.25–1.75	1	2	4	2	2	11
1.75–2.25	0	0	5	1	0	6
2.25–2.75	2	0	5	0	0	7
> 2.75	1	0	3	0	0	4
Total	20	25	33	6	7	91

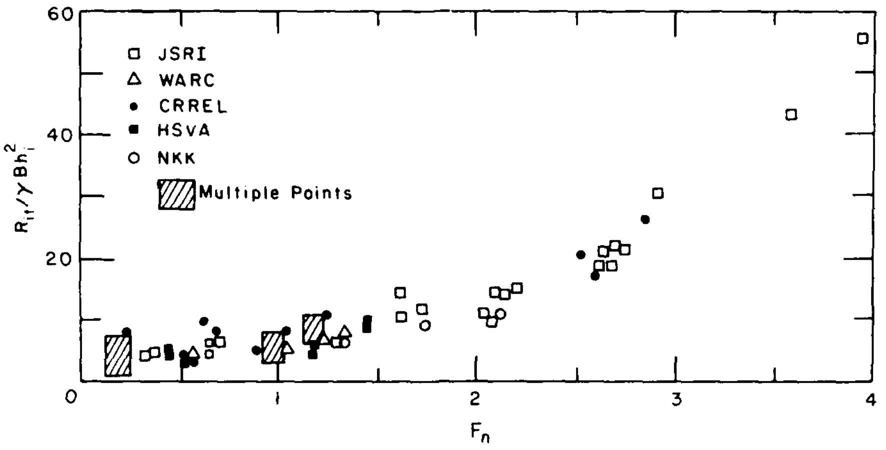

a. Data points for full range of F_n.

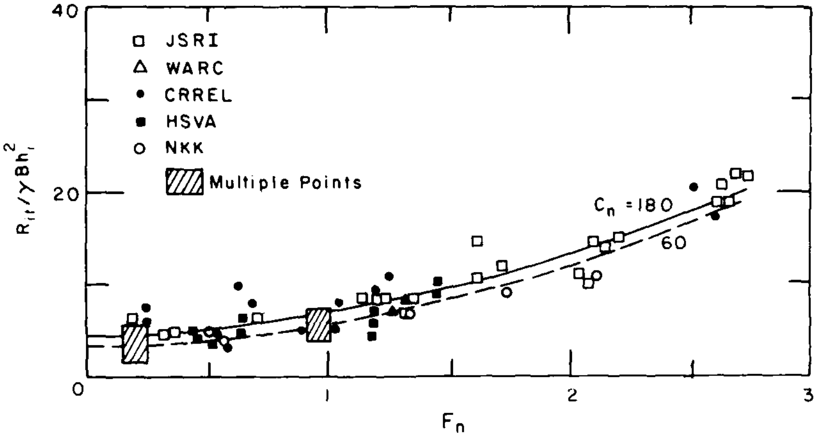

b. Form II of regression equation for $F_n < 3$.

Figure 13. Comparison of resistance data with smooth R-class model from all facilities.

$C \cdot C_n$. The values of the coefficients A, B and C are listed in Table 14b for both the total and net resistance.

From the results of the regression analyses with form I and form II, it can be seen that the CRREL test results show a somewhat greater dependence of R_* on C_n than do those from both JSRI and HSVA. Consequently, CRREL data yield a smaller value of the intercept A of both forms of the regression equation as compared to the intercepts obtained for the HSVA and JSRI data.

The results of these analyses are presented graphically for each facility in Figure 13b, where form II of the regression equation was plotted for the extreme values $C_n = 60$ and $C_n = 180$ of the range of C_n called for in the initial test program. In Figure 14, the results from all the facilities are presented as the measured values of R_* plotted against the values calculated by form II of the regression equation for the actual test conditions. The data from all facilities are in very reasonable agreement with one another, as can be seen from Figure 14 where it is shown that 67 data points out of a total of 87 (i.e., 77%) fall within ±25% of the predictions.

Table 14. Results of regression analysis of resistance tests from all facilities (smooth model; F_n<2.75).

a. Form I: $R_* = A + B \cdot F_n + C \cdot F_n^2 + D \cdot C_n$

Laboratory	A	B	C	D	r
			Total Resistance		
CRREL	0.066	0.917	1.461	0.0375	0.980
(90% C.I.)	±1.425	±1.982	±0.720	±0.0091	
HSVA	2.070	−0.002	2.182	0.0152	0.918
(90% C.I.)	±1.090	±2.929	±1.917	±0.0071	
JSRI	2.685	0.785	1.944	0.0062	0.976
(90% C.I.)	±1.367	±1.895	±0.661	±0.0037	
NKK	Insufficient range for C_n				
WARC	Insufficient data range				
All labs	2.717	0.450	1.962	0.0090	0.959
(90% C.I.)	±0.708	±1.115	±0.417	±0.0028	
			Net Resistance		
CRREL	0.19	1.09	0.78	0.0364	0.966
(90% C.I.)	±1.41	±1.96	±0.71	±0.0090	
HSVA	2.04	0.63	1.242	0.0142	0.882
(90% C.I.)	±1.06	±2.84	±1.86	±0.0069	
JSRI	3.06	0.94	1.22	0.0042	0.968
(90% C.I.)	±1.11	±1.54	±0.54	±0.0030	
All labs	2.87	0.73	1.23	0.0073	0.971
(90% C.I.)	±0.65	±1.03	±0.417	±0.0026	

b. Form II: $R_* = A + B \cdot F_n^2 + C \cdot C_n$

Laboratory	A	B	C	r
		Total Resistance		
CRREL	0.413	1.777	0.0379	0.980
(90% C.I.)	±1.192	±0.217	±0.0089	
HSVA	2.070	2.181	0.0152	0.918
(90% C.I.)	±0.712	±0.403	±0.0069	
JSRI	3.086	2.209	0.0060	0.977
(90% C.I.)	±0.954	±0.163	±0.0036	
All labs	2.930	2.122	0.0089	0.959
(90% C.I.)	±0.470	±0.121	±0.0028	
		Net Resistance		
CRREL	0.60	1.15	0.0367	0.964
(90% C.I.)	±1.19	±0.22	±0.0089	
HSVA	2.21	1.64	0.0140	0.881
(90% C.I.)	±0.69	±0.39	±0.0067	
JSRI	3.54	1.54	0.0040	0.967
(90% C.I.)	±0.78	±0.13	±0.0030	
All labs	3.22	1.49	0.0072	0.933
(90% C.I.)	±0.44	±0.11	±0.0026	

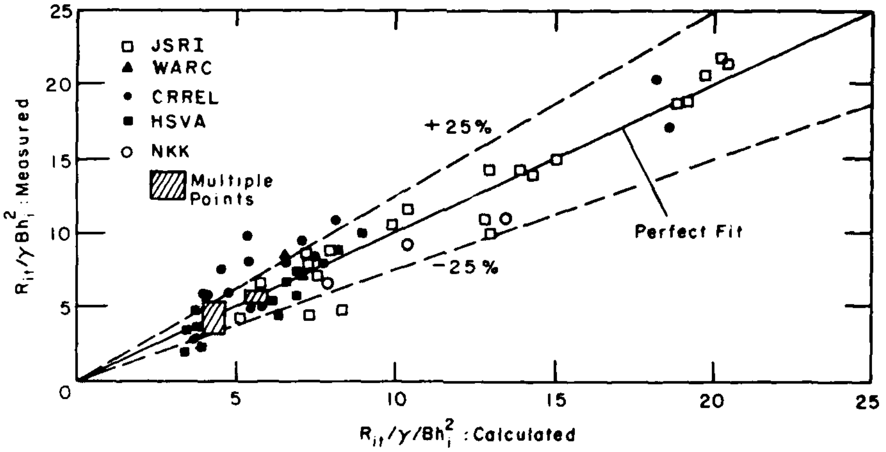

Figure 14. Measured vs calculated total resistance (form II of regression function).

Propulsion tests

Four facilities, namely CRREL, HSVA, JSRI and WARC, carried out propulsion tests with the smooth 1:20 scale R-class model, the results of which were part of the report by the Ice Committee at the 17th ITTC (ITTC 1984). Only the tests run at HSVA were made with a free-running model; it was connected to the main carriage by only an umbilical cord for power supply and data transmission. The other three facilities carried out the tests by the captive model technique. At JSRI the propeller speed was adjusted during the tests to attain the self-propulsion point, i.e., so that the net average towing force or pull would be zero. Finally, the tests at WARC were performed in previously sawn ice. The model was towed by the carriage at predicted speed and propeller rpm for the particular conditions of thickness and strength of the parent ice sheet, while the pull exerted by the towing mechanism, and propeller thrust and torque were measured. The writers are not familiar with the test technique used by WARC and are unsure whether the WARC data presented in the Committee report should be interpreted as being at self-propulsion points or not.

The data for the self-propulsion tests at HSVA and JSRI, the published test data of WARC and the self-propulsion test points derived from the captive model tests at CRREL (as explained in a previous section of the present report) are listed in Table A2. The thrust deduction factor, t, was calculated as

$$t = 1 - R_p / T_a. \tag{26}$$

where R_p is the total ice resistance for the test conditions of velocity, ice thickness and ice strength predicted using form I of the resistance regression equation for the resistance tests from all facilities. T_a is the measured average thrust.

Plots of the thrust, K_t, and torque, K_q, coefficients in Figures 15a and b, respectively, against the apparent advance coefficient, J_a, show a linear relationship:

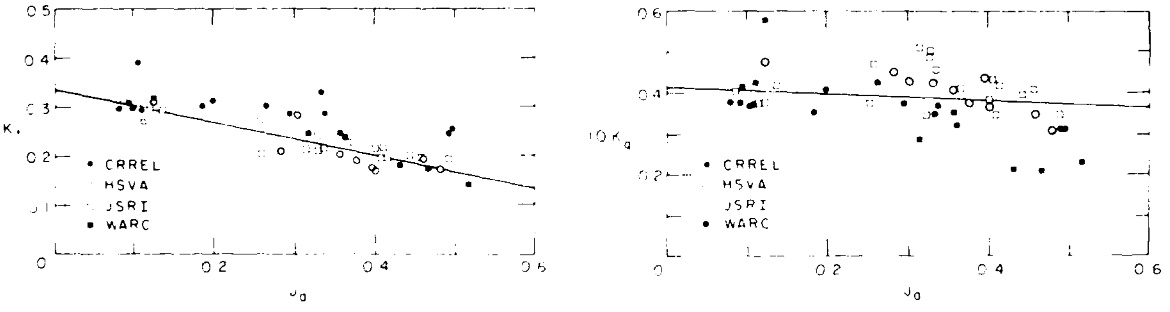

a. Thrust coefficient, K_t, *vs apparent advance coefficient,* J_a.

b. Torque coefficient, K_q, *vs apparent advance coefficient,* J_a.

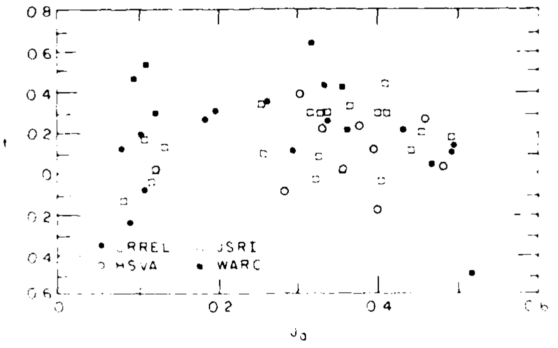

c. Thrust deduction factor, t, *vs apparent advance coefficient,* J_a.

Figure 15. Comparison of propulsion test results with smooth model.

$$K_t, K_q = A - B \cdot J_a. \tag{27}$$

As seen from Figure 15a, the thrust coefficient measured in the CRREL tests appears to be consistently greater than for any other laboratory, which does confirm the suspicion held during the tests that the thrust dynamometers were not functioning properly. Similarly, from Figure 15b it can be seen that the torque coefficients measured at WARC are off with respect to the results from the other facilities. Therefore, the combined data were analyzed with and without those particular tests, and the results listed in Table 15 and shown graphically on Figure 15.

The thrust deduction factor, t, calculated according to eq 26 is plotted against J_a in Figure 15c. No obvious variation of t with J_a is apparent, and for the range of test conditions at all facilities the average thrust deduction factor is equal to 0.168. Another approach is to plot the predicted resistance, R_p, against the measured average total thrust, T_a, as in Figure 16, which shows a linear relationship between these two quantities. Under the assumption that

$$R_p + dR = [1-(t + dt)]T_a \tag{28}$$

where dR is the uncertainty on R_p at the 90% confidence interval and dt the corresponding uncertainty on t, it was found that $t = 0.184 \pm 0.094$.

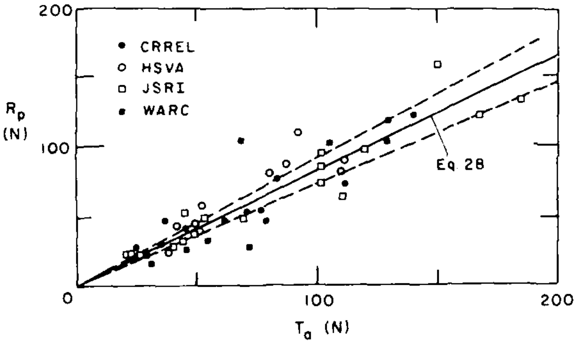

Figure 16. Predicted resistance of smooth model vs total thrust measured during propulsion tests.

Table 15. Results of linear regression analysis on K_t and K_q (smooth R-class model; all laboratories).

Laboratory	A	B	r
a. Thrust coefficient: $K_t = A - B \cdot J_a$			
CRREL	0.337	0.152	0.624
(90% C.I.)	±0.032	±0.110	
HSVA	0.356	0.408	0.865
(90% C.I.)	±0.058	±0.159	
JSRI	0.324	0.297	0.918
(90% C.I.)	±0.018	±0.054	
WARC	0.338	0.338	0.933
(90% C.I.)	±0.033	±0.096	
All labs	0.341	0.320	0.797
(90% C.I.)	±0.020	±0.059	
All labs except CRREL	0.334 ±0.015	0.332 ±0.044	0.904
b. Torque coefficient: $K_q = A - B \cdot J_a$			
CRREL	0.0397	0.0144	0.634
(90% C.I.)	±0.0029	±0.0102	
HSVA	0.0553	0.0445	0.862
(90% C.I.)	±0.0064	±0.0175	
JSRI	0.0410	0.0012	0.029
(90% C.I.)	±0.0059	±0.0174	
WARC	0.0537	0.0669	0.875
(90% C.I.)	±0.0093	±0.0271	
All labs	0.0448	0.0221	0.416
(90% C.I.)	±0.0039	±0.0117	
All labs except WARC	0.0415 ±0.0034	0.0080 ±0.0102	0.206

Tests with roughened model

Resistance tests

All six facilities (CRREL, HSVA, JSRI, NKK, NRCC and WARC) reported the results of their resistance tests with the roughened R-class model at the 18th ITTC, October 1987, Kobe, Japan (ITTC 1987). These test results are given in Table A3. Results of regression analyses of the total resistance data with forms I and II of the regression equation are presented in Table 16. The results of the analysis of the net resistance data with form I of the regression equation, Table 17a, showed that the contribution of the term in F_n^2 was negligible,

Table 16. Results of regression analysis on total resistance data with roughened model.

Laboratory	A	B	C	D	r
a. Form I: $R_* = A + B \cdot F_n + C \cdot F_n^2 + D \cdot C_n$					
CRREL	2.68	2.50	1.00	0.0174	0.961
(90% C.I.)	±2.01	±1.97	±0.70	±0.0132	
NRCC	0.06	4.93	0.42	0.0345	0.978
(90% C.I.)	±2.53	±2.88	±1.03	±0.0207	
NKK	3.17	−0.50	−2.16	−0.0247	0.999
(90% C.I.)	±3.01	±2.68	±1.05	±0.0211	
JSRI	0.96	3.44	0.91	0.0316	0.989
(90% C.I.)	±1.27	±1.41	±0.51	±0.0085	
HSVA	2.19	1.39	2.18	0.0186	0.987
(90% C.I.)	±2.00	±2.68	±0.99	±0.0128	
WARC	2.42	2.54	3.80	0.0304	0.988
(90% C.I.)	±1.69	±3.37	±1.98	±0.0098	
All except WARC	1.41	2.73	1.15	0.0272	0.966
(90% C.I.)	±1.00	±1.11	±0.40	±0.0064	
b. Form II: $R_* = A + B \cdot F_n^2 + C \cdot C_n$					
CRREL	4.21	1.86	0.0155	—	0.954
(90% C.I.)	±1.71	±0.19	±0.0140		
NRCC	3.09	2.12	0.0300	—	0.958
(90% C.I.)	±2.34	±0.35	±0.0176		
NKK	2.85	1.97	0.0254	—	0.984
(90% C.I.)	±2.32	±0.26	±0.0194		
JSRI	2.40	2.11	0.0339	—	0.978
(90% C.I.)	±1.53	±0.19	±0.0116		
HSVA	2.84	2.67	0.0184	—	0.986
(90% C.I.)	±1.54	±0.25	±0.0126		
WARC	3.38	5.25	0.0277	—	0.987
(90% C.I.)	±1.15	±0.42	±0.0093		
All except WARC	2.87	2.11	0.0264	—	0.959
(90% C.I.)	±0.87	±0.11	±0.0069		

and a form III of the equation, linear in both F_n and C_n, was also applied and the corresponding coefficients listed in Table 17b.

The nondimensional total resistance data are plotted in Figure 17a. Note that the WARC data points are distinctly higher than those from all the other laboratories. In this respect, the following should be recognized: 1) WARC was the first facility to test the roughened model and it is possible that this first series of tests somewhat smoothed the model so that the friction factor was greater at WARC than at any other facility, and 2) between the tests with the smooth model and those with the roughened one, WARC changed its model ice from the columnar saline type to the fine-grain type and found out that the ship models had

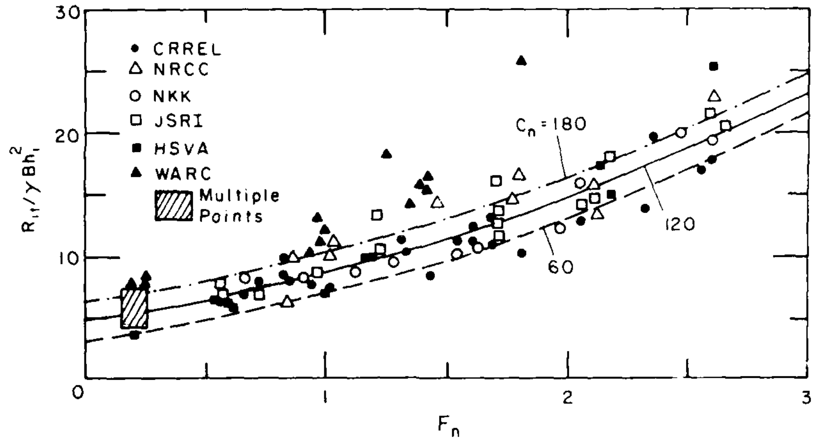

a. Total resistance vs Froude number.

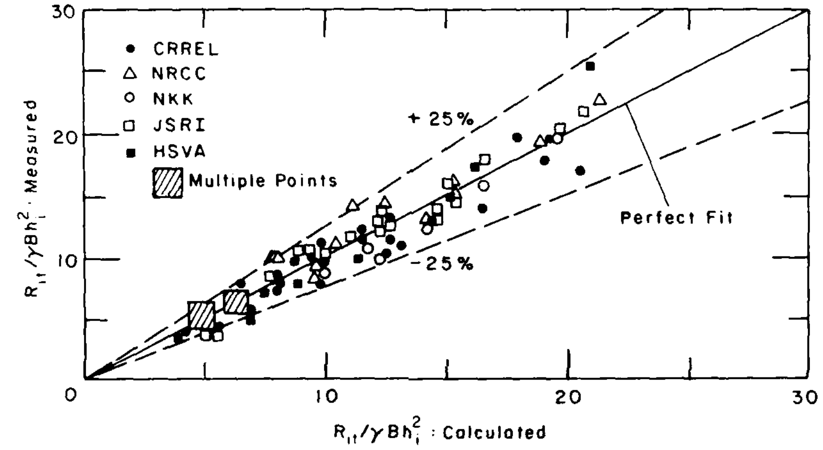

b. Measured vs calculated total resistance.

Figure 17. Resistance tests with roughened R-class model at participating facilities.

to have a lower friction coefficient with the new ice to have the same resistance as in the previous model ice. For these reasons, WARC data were not included when performing the regression analyses on all available test data. The corresponding regression line (form I of the equation) is also shown in Figure 17a. Figure 17b presents the comparison between the resistance given by the regression equation derived and that measured at all facilities except WARC. It can be seen that all data points fall within ± 25% of the calculated values.

Propulsion tests

Only three facilities, namely CRREL, JSRI and NRCC, have reported results of propulsion tests with the roughened model, the results of which are listed in Table A4.

The thrust and torque coefficients, K_t and K_q, are plotted against the apparent advance coefficient J_a on Figure 18, and the results of the linear regression analyses of K_t and K_q according to eq 28 are listed in Table 18. The regression line for all laboratories is shown on Figure 18. It can be observed that the results on K_t and K_q obtained at the various facilities are in excellent agreement with one another, and comparison with the data obtained with

Table 17. Results of regression analysis on net resistance data with roughened model.

Laboratory	A	B	C	D	r
a. Form I : $R_* = A + B \cdot F_n + C \cdot F_n^2 + D \cdot C_n$					
CRREL	2.74	2.91	0.22	0.0157	0.944
(90% C.I.)	±1.64	±1.61	±0.57	±0.0108	
NRCC	0.32	5.29	–0.30	0.0314	0.966
(90% C.I.)	±2.37	±2.70	±0.097	±0.0130	
NKK	4.06	–0.15	1.52	0.0162	0.976
(90% C.I.)	±2.75	±2.45	±0.96	±0.0192	
JSRI	1.26	4.09	0.06	0.0272	0.990
(90% C.I.)	±0.92	±1.02	±0.37	±0.0062	
HSVA	2.32	1.75	1.49	0.0162	0.987
(90% C.I.)	±1.62	±2.18	±0.80	±0.0104	
WARC	2.51	3.24	2.80	0.0285	0.988
(90% C.I.)	±1.49	±2.97	±1.74	±0.0086	
All except WARC	1.59	3.19	0.38	0.0244	0.946
(90% C.I.)	±0.93	±1.03	±0.38	±0.0059	
b. Form III: $R_* = A + B \cdot F_n + C \cdot C_n$					
CRREL	2.41	3.50	0.0162	—	0.943
(90% C.I.)	±1.37	±0.41	±0.0106		
NRCC	0.77	4.49	0.0306	—	0.965
(90% C.I.)	±1.79	±0.68	±0.0122		
NKK	1.48	3.57	0.0244	—	0.949
(90% C.I.)	±2.99	±0.89	±0.0249		
JSRI	1.20	4.25	0.0271	—	0.990
(90% C.I.)	±0.82	±0.26	±0.0060		
HSVA	0.51	5.66	0.0182	—	0.973
(90% C.I.)	±1.76	±0.76	±0.0140		
WARC	0.83	7.91	0.0337	—	0.981
(90% C.I.)	±1.29	±0.75	±0.0097		
All except WARC	1.08	4.21	0.0249	—	0.944
(90% C.I.)	±0.79	±0.27	±0.0060		

the smooth model shows no significant effect of the hull roughness on the thrust and torque coefficients.

The thrust deduction factor, *t*, was calculated by eq 26 where R_p is the total ice resistance given by form I of the resistance equation, namely

$$R_p/\gamma B h_i^2 = 1.413 + 2.73\, F_n + 1.149\, F_n^2 + 0.0272\, C_n \tag{29}$$

and is plotted versus J_a on Figure 19. Considering the inherent uncertainty in values of *t* for tests in ice, there is remarkable agreement between the three laboratories. In contrast with

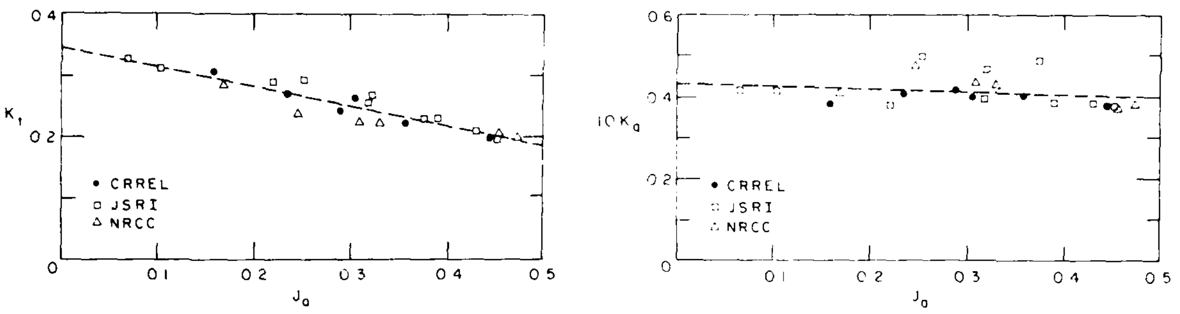

a. Thrust coefficient, K_t*, vs apparent advance coefficient,* J_a*.*

b. Torque coefficient, K_q*, vs apparent advance coefficient,* J_a*.*

Figure 18. Comparison of propeller coefficients from propulsion test results with roughened model.

the results for the smooth model, the scatter in t is relatively moderate and, in particular, there are no negative values. There is no evident effect of J_a on t, which can be considered constant, equal to 0.182 with a standard deviation of 0.073. This is identical to the result of $t = 0.184 \pm 0.094$ obtained for the smooth model.

Another way of determining t is to plot the total resistance predicted by eq 29 against the corresponding measured total thrust, T_a, as in Figure 19b. Linear regression of these data yielded $t = 0.178$ with a 90% confidence interval of ±0.021, equivalent to the previous result.

Comparison with full-scale data

As noted earlier, the values of the propeller coefficients, K_t and K_q, obtained from model tests with both the smooth and roughened models were nearly identical. In Figure 20, these model test values are compared with full-scale data calculated from the measurements presented by Michailidis and Murdey (1981) and with results from model tests in clear water (Murdey 1980). It can be seen that the values of K_t obtained in both types of model tests, i.e., in level ice and in clear water, are practically identical and match well the full-scale values, especially for $J_a > 0.25$, approximately. For $J_a < 0.2$, the full scale values of K_t are somewhat lower than those obtained in model tests. On the other hand, the values of the torque coefficient, K_q, measured in model tests in level ice are consistently greater than those measured in clear water tests, and the latter are in excellent agreement with the full scale values of K_q.

The ship performance at full power predicted from model test results are presented in Figure 21 as maximum velocity versus ice thickness for an assumed value of 450 kPa of the ice strength, the average of σ_i reported by Michailidis and Murdey. Figure 21 also shows the full-scale data reported by Michailidis and Murdey and those presented in the 1987 ITTC Ice Committee report (ITTC 1987) based on all available

Table 18. Results of linear regression analysis on K_t and K_q (roughened R-class model; all facilities).

Laboratory	A	B	r
a. Thrust coefficient: $K_t = A - B \cdot J_a$			
CRREL (90% C.I.)	0.358 ±0.037	0.365 ±0.117	0.965
JSRI (90% C.I.)	0.354 ±0.016	0.326 ±0.051	0.974
NRCC (90% C.I.)	0.304 ±0.038	0.232 ±0.109	0.929
All labs (90% C.I.)	0.344 ±0.015	0.319 ±0.047	0.936
b. Torque coefficient: $K_q = A - B \cdot J_a$			
CRREL (90% C.I.)	0.0402 ±0.0052	0.0026 ±0.0166	0.178
JSRI (90% C.I.)	0.0425 ±0.0075	0.0031 ±0.0234	0.087
NRCC (90% C.I.)	0.0484 ±0.0102	0.0211 ±0.0295	0.644
All labs (90% C.I.)	0.0432 ±0.0040	0.0072 ±0.0124	0.220

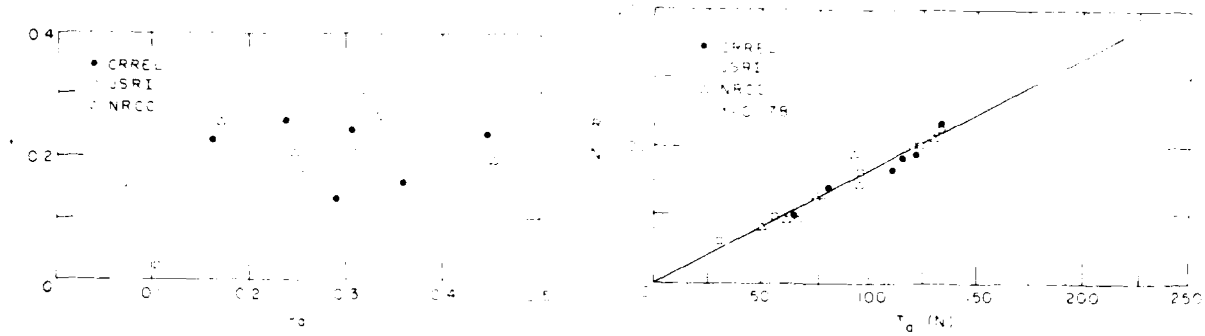

a. Calculated by eq 26.

b. From plot of R_p versus T_a.

Figure 19. Thrust deduction factor.

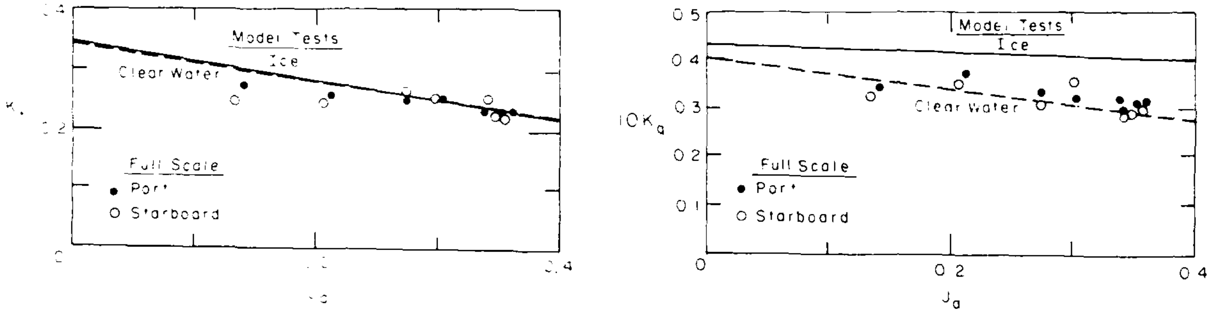

a. Thrust coefficient, K_t, vs apparent advance coefficient, J_a.

b. Torque coefficient, K_q, vs apparent advance coefficient, J_a.

Figure 20. Comparison between model test results and full-scale data.

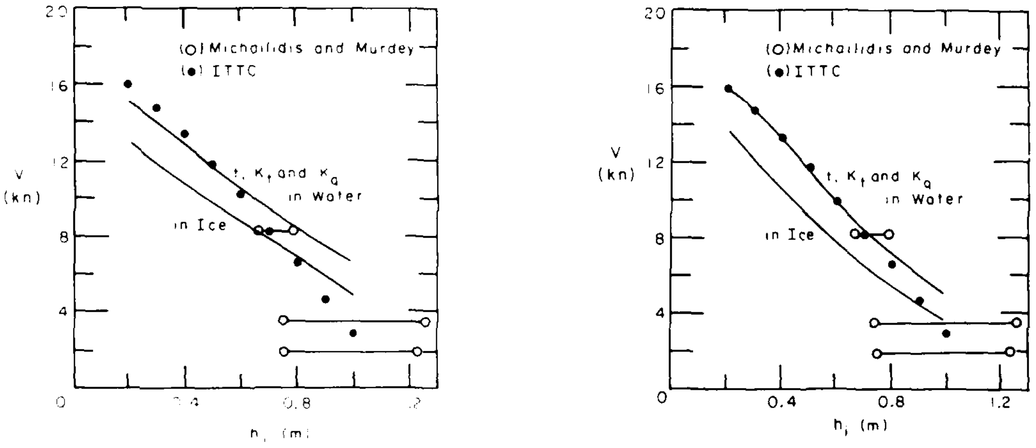

a. Based on smooth model test results.

b. Based on roughened model test results.

Figure 21. Comparison between predicted performance in level ice and full-scale measurements (σ_i = 450 kPa).

reports of field trials with the R-class icebreakers. It should be noted that the thickness interval indicated by a solid line segment on Figure 21 for the data of Michailidis and Murdey represents the thickness of the snow layer overlaying the sheet ice. The ship performance predictions were calculated from the model test results with both the smooth (Fig. 21a) and rough (Fig. 21b) models, and using the values of K_t, K_q and t obtained from model test in both level ice and clear water. From Figure 21, it can be concluded that:

1. The predictions based on the resistance tests results with the rough model match the full-scale trial data better than those based on resistance tests results with the smooth model.

2. For ice thickness less than 0.7 m, the "rough model" predictions based on propeller coefficients from tests in clear water are in near-perfect agreement with the full-scale measurements. As the ice thickness increases beyond 0.7 m, and the maximum ship speed at full power decreases accordingly, the full-scale data agree more and more with the predictions based on propeller coefficients from model tests in level ice. This observation confirms the concern that model propulsion tests in level ice performed in relatively thin level ice, or at high speed, yield propeller coefficients that are too pessimistic.

3. For the field conditions documented on Figure 21, the effect of snow on the ship performance can be accounted for by increasing the ice thickness by half the snow thickness.

CONCLUSIONS AND RECOMMENDATIONS

CRREL tests

Following resistance and propulsion tests in level ice with a smooth (friction factor of about 0.04) model of the R-class icebreaker, similar tests were performed with a roughened model. From the results of these tests the following observations can be made.

1. The ice friction tests indicated that the apparent friction coefficient, f_a, defined as the *ratio of the tangential force*, T, to the normal load, N, decreases with increasing N. In other words, the tangential force is not directly proportional to the normal load but a linear function of it. The intercept, T_o, was interpreted as an adhesion stress, the exact origin of which remains to be clarified, while the slope was interpreted as the actual friction coefficient. The friction factor of the original "smooth" model had been measured at 0.04; that of the roughened model was approximately 0.07.

2. The increase in nondimensional resistance due to the increase in the friction coefficient decreased with increasing nondimensional ice strength, C_n. For $C_n = 60$, the resistance of the roughened model was 10 to 20% greater than that of the smooth model, while for $C_n =$ 180 the resistance of both models was nearly the same.

3. The propeller characteristics, K_t, K_q and t, of both models were practically identical, showing no effect of the increase in hull roughness.

Comparative studies

Both models had been tested by several research facilities both in resistance and in propulsion. Comparison of the test results between these facilities can be summarized as follows.

1. For the most part, the resistance and propulsion test results from any facility fall within ±25% of the overall average test results. Furthermore, for given test conditions of ice thickness, ice strength and ship speed, the variation in test results between research facilities is of the same order as that at any one facility.

2. The model propulsion test results of all facilities showed that the propeller thrust coefficient in level ice was practically the same as in clear water, while the torque coefficient in level ice was nearly constant and significantly greater than in clear water. Significant uncertainty in the thrust deduction factor, especially with the smooth model, deduced from

the results of propulsion tests in level ice has to be attributed primarily to unavoidable uncertainty in the model resistance test results. Overall, the thrust deduction factor in level ice was found to be approximately constant, equal to 0.18 ± 0.07, rather than increasing with ship speed (or apparent advance coefficient) as in clear water.

3. Ship performance prediction presented as maximum ship speed versus ice thickness based on roughened model resistance and propeller characteristics in clear water showed excellent agreement with available full-scale trials data for ice thickness up to 0.7 m. For thicker ice, good comparisons were obtained when the propeller characteristics from tests in ice were used in the prediction algorithms. These observations would seem to indicate that, compared to full scale, ice effect on propulsion is exaggerated in model tests at relatively high speed in ice of low to medium thickness, but is correctly modeled in tests in thick ice.

It is extremely encouraging to find that ship testing in ice has reached a level of reliability where different facilities, using somewhat different model ice and slightly different testing techniques, obtain overall results that are comparable, both in resistance and propulsion, with an uncertainty in the results that, in the opinion of the writers, is inherent to the icebreaking phenomenon. However, progress in the development of model ice, modeling techniques, and data analysis and interpretation is still needed, especially concerning ice–propeller interaction, which is usually exaggerated at the model scale. This area of research is one that is and ought to be receiving further attention from all ice research facilities in order to achieve a level of confidence in the results of model tests in ice and their extrapolation to full scale comparable to that enjoyed by model tests in a traditional, open-water towing tank.

LITERATURE CITED

Edwards, R. Y., M. A. Dunne, G. Comfort, V. Bulat and B. Johnson (1981) Results of full-scale trials in ice of CCG *Pierre Radisson. Proceedings, Sixth Ship Technology and Research (STAR) Symposium, 17–19 June, Ottawa, Canada.* New York: The Society of Naval Architects and Marine Engineers, p. 291–310.

Forland, K. and J. C. Tatinclaux (1985) Kinetic friction coefficient of ice. USA Cold Regions Research and Engineering Laboratory, CRREL Report 85-6.

ITTC (1981) Report of the Committee on Performance of Ships in Ice-Covered Waters. *Proceedings, 16th International Towing Tank Conference, 31 August–9 September, Leningrad, USSR.* Vol. I. Krylov Ship Research Institute, p. 363–376.

ITTC (1984) Report of the Committee on Performance of Ships in Ice-Covered Waters. *Proceedings, 17th International Towing Tank Conference, 8–15 September, Göteborg, Sweden.* Vol. I. Swedish Maritime Research Center (SSPA), p. 589–625.

ITTC (1987) Report of the Committee on Performance of Ships in Ice-Covered Waters. *Proceedings, 18th International Towing Tank Conference, 18–24 October, Kobe, Japan.* Vol. I. The Society of Naval Architects of Japan, p. 527–566.

Michailidis, M. and D. C. Murdey (1981) Performance of CCGS *Franklin* in Lake Melville, 1980. *Proceedings, Sixth Ship Technology and Research (STAR) Symposium, 17–19 June, Ottawa, Canada.* New York: The Society of Naval Architects and Marine Engineers, p. 311–322.

Murdey, D. C. (1980) Resistance and propulsion experiments with model 327-1 and propellers 66L and 66R. Technical Report No. LTR-SH-269, National Research Council, Division of Mechanical Engineering, Ottawa, Canada.

Tatinclaux, J. C. (1984) Model tests in ice of a Canadian Coast Guard R-class icebreaker. USA Cold Regions Research and Engineering Laboratory, Special Report 84-6.

APPENDIX A: TEST RESULTS (ALL LABORATORIES)

Table A1. Resistance test results with smooth model.
a. Dimensional data.

h (mm)	σ (kPa)	V (m/s)	R_T (N)
[illegible]			
[illegible]	[illegible]	[illegible]	[illegible]
[illegible]	45.0	[illegible]	[illegible]
[illegible]	[illegible]	[illegible]	[illegible]
[illegible]	[illegible]	[illegible]	[illegible]
[illegible]	[illegible]	[illegible]	[illegible]
[illegible]	47.0	[illegible]	47.0
[illegible]	[illegible]	[illegible]	[illegible]
[illegible]	[illegible]	[illegible]	[illegible]
[illegible]	[illegible]	[illegible]	[illegible]
[illegible]	[illegible]	[illegible]	[illegible]
[illegible]	47.0	[illegible]	[illegible]
[illegible]	34.0	[illegible]	[illegible]
[illegible]	[illegible]	[illegible]	44.4
[illegible]	[illegible]	[illegible]	[illegible]
[illegible]	[illegible]	[illegible]	[illegible]
[illegible]	[illegible]	[illegible]	45.4
[illegible]	47.0	[illegible]	[illegible]
[illegible]	45.0	[illegible]	39.0
[illegible]	[illegible]	[illegible]	[illegible]
[illegible]	55.0	[illegible]	[illegible]
[illegible]			
[illegible]	[illegible]	[illegible]	[illegible]
43.0	[illegible]	[illegible]	[illegible]
[illegible]	[illegible]	[illegible]	[illegible]
[illegible]	40.0	[illegible]	[illegible]
[illegible]	[illegible]	[illegible]	[illegible]
[illegible]	[illegible]	[illegible]	[illegible]
26.0	[illegible]	[illegible]	[illegible]
[illegible]	[illegible]	[illegible]	[illegible]
[illegible]	[illegible]	[illegible]	[illegible]
[illegible]	[illegible]	[illegible]	14.0
[illegible]	[illegible]	[illegible]	[illegible]
74.0	40.0	[illegible]	[illegible]
26.0	[illegible]	[illegible]	[illegible]
[illegible]	[illegible]	[illegible]	[illegible]
[illegible]	[illegible]	[illegible]	[illegible]
[illegible]	[illegible]	[illegible]	[illegible]
[illegible]	[illegible]	[illegible]	[illegible]
[illegible]	[illegible]	[illegible]	[illegible]
[illegible]	43.0	[illegible]	[illegible]
[illegible]	[illegible]	[illegible]	[illegible]
[illegible]	40.0	[illegible]	[illegible]
[illegible]	25.0	[illegible]	[illegible]
[illegible]	[illegible]	[illegible]	[illegible]
[illegible]	[illegible]	[illegible]	[illegible]
[illegible]	[illegible]	[illegible]	[illegible]

h (mm)	σ (kPa)	V (m/s)	R_T (N)
[illegible]			
[illegible]	43.5	[illegible]	[illegible]
[illegible]	[illegible]	[illegible]	[illegible]
[illegible]	55.0	[illegible]	[illegible]
[illegible]	[illegible]	[illegible]	[illegible]
[illegible]	[illegible]	[illegible]	[illegible]
[illegible]	[illegible]	[illegible]	[illegible]
[illegible]	44.4	[illegible]	[illegible]
[illegible]	[illegible]	[illegible]	[illegible]
8.4	[illegible]	[illegible]	4.4
[illegible]	[illegible]	[illegible]	[illegible]
[illegible]	[illegible]	[illegible]	[illegible]
[illegible]	[illegible]	[illegible]	[illegible]
[illegible]	[illegible]	[illegible]	46.0
[illegible]	[illegible]	[illegible]	[illegible]
[illegible]	[illegible]	[illegible]	[illegible]
[illegible]	36.5	[illegible]	[illegible]
[illegible]	[illegible]	[illegible]	[illegible]
[illegible]	[illegible]	[illegible]	[illegible]
[illegible]	[illegible]	[illegible]	[illegible]
[illegible]	[illegible]	[illegible]	48.4
[illegible]	[illegible]	[illegible]	[illegible]
[illegible]	[illegible]	[illegible]	[illegible]
[illegible]	[illegible]	[illegible]	[illegible]
[illegible]	[illegible]	[illegible]	[illegible]
[illegible]	[illegible]	[illegible]	[illegible]
[illegible]	[illegible]	[illegible]	[illegible]
[illegible]	[illegible]	[illegible]	44.4
[illegible]	45.4	[illegible]	[illegible]
[illegible]	[illegible]	[illegible]	[illegible]
[illegible]	[illegible]	[illegible]	[illegible]
[illegible]	[illegible]	[illegible]	[illegible]
[illegible]	[illegible]	[illegible]	[illegible]
[illegible]	[illegible]	[illegible]	[illegible]
[illegible]			
35.6	[illegible]	[illegible]	[illegible]
[illegible]	[illegible]	[illegible]	44.4
75.0	[illegible]	0.564	[illegible]
35.5	[illegible]	[illegible]	[illegible]
[illegible]	[illegible]	[illegible]	[illegible]
[illegible]	[illegible]	[illegible]	[illegible]
[illegible]			
[illegible]	[illegible]	[illegible]	[illegible]
[illegible]	[illegible]	[illegible]	[illegible]
[illegible]	[illegible]	[illegible]	[illegible]
[illegible]	[illegible]	[illegible]	[illegible]
[illegible]	[illegible]	[illegible]	[illegible]
[illegible]	[illegible]	[illegible]	[illegible]
[illegible]	[illegible]	[illegible]	[illegible]

Table A1 (cont'd). Resistance test results with smooth model.
b. Nondimensional data.

F_n	C_u	$R_{it}/\gamma Bh_i^2$	$R_i/\gamma Bh_i^2$
	CRREL		
0.19	70.2	2.75	2.70
0.22	103.3	5.70	5.69
0.22	70.6	3.58	3.56
0.24	103.3	5.67	5.62
0.24	132.0	5.77	5.72
0.25	158.7	7.43	7.39
0.26	140.2	4.87	4.81
0.54	90.9	4.43	4.21
0.59	62.7	3.29	3.15
0.60	179.7	9.61	9.41
0.72	159.7	7.92	7.56
0.90	97.6	4.94	4.63
1.03	59.6	5.06	4.62
1.05	142.6	9.21	7.53
1.19	131.2	9.29	9.26
1.23	160.7	8.01	7.25
1.28	212.9	10.71	9.64
2.52	202.1	20.23	15.06
2.61	145.2	7.07	12.97
2.99	260.9	25.92	20.29
	HSVA		
0.16	55.0	3.11	3.09
0.17	69.5	4.64	4.62
0.18	52.3	1.82	1.80
0.18	116.5	2.51	2.47
0.19	70.9	3.01	3.03
0.19	116.1	4.32	4.29
0.20	70.9	3.52	3.46
0.21	99.1	3.53	3.50
0.23	117.9	4.22	4.13
0.45	69.5	4.99	4.32
0.45	54.0	3.91	3.54
0.52	118.9	4.25	4.17
0.52	116.1	4.91	4.29
0.52	70.6	4.15	4.07
0.53	51.0	3.01	3.03
0.64	97.3	4.43	4.14
0.65	161.7	5.24	5.75
0.99	54.2	5.17	4.88
1.01	69.5	5.79	5.46
1.19	51.2	4.26	3.65
1.19	118.2	5.63	5.01
1.19	72.9	5.60	5.22
1.19	116.1	7.32	6.77
1.45	95.1	9.64	7.44
1.45	181.7	9.83	9.44

F_n	C_u	$R_{it}/\gamma Bh_i^2$	$R_i/\gamma Bh_i^2$
	USCG		
0.19	118.2	4.67	4.66
0.19	100.2	2.75	2.74
0.19	187.7	6.26	6.25
0.24	150.9	3.61	3.47
0.24	240.7	6.27	6.23
0.24	124.4	3.43	3.39
0.25	217.2	4.17	4.12
0.33	457.9	4.23	4.29
0.36	572.5	4.72	4.51
0.71	196.2	6.22	5.96
0.84	23.4	5.64	5.16
0.84	122.2	6.94	5.66
1.19	156.9	9.46	7.61
1.22	206.3	8.71	7.64
1.23	139.0	7.94	6.79
1.24	92.2	9.09	6.86
1.32	120.9	7.04	6.20
1.62	499.2	14.25	11.22
1.62	156.8	10.25	8.71
1.72	29.2	1.42	3.01
2.24	118.2	10.67	9.01
2.26	122.2	9.70	7.91
2.29	157.7	14.13	12.29
2.32	188.2	10.91	9.61
2.32	206.7	14.97	11.47
2.61	150.9	18.69	14.03
2.62	240.7	20.62	16.93
2.66	124.4	18.66	13.43
2.69	217.3	21.61	16.66
2.77	190.2	21.29	15.93
2.91	499.2	32.50	20.12
3.55	457.9	42.98	27.24
3.95	572.5	55.22	31.90
	NRC		
0.19	124.6	3.05	3.04
0.58	115.6	3.93	3.70
0.96	115.3	5.22	4.83
1.34	124.9	6.67	6.60
1.75	114.1	8.59	7.59
2.12	118.5	12.75	9.85
	WARC		
0.36	72.8	5.68	5.27
0.38	79.2	6.54	6.22
0.39	92.6	6.52	6.11
1.05	38.6	5.40	4.97
1.17	49.7	8.27	7.64
1.27	39.2	7.21	6.30
1.24	127.7	9.06	7.50

Table A2. Self-propulsion points of smooth model.
a. Dimensional data.

h_i (mm)	σ_i (kPa)	V (m/s)	n_a (rpm)	T_a (N)	Q_a (Nm)	R_p (N)
			CRREL			
27.3	33.5	0.110	305	26.0	0.72	28.6
27.3	24.0	0.110	293	25.0	0.65	26.2
37.0	22.0	0.110	348	37.0	0.82	44.6
32.5	36.5	0.110	394	45.0	1.20	29.7
36.7	25.0	0.310	488	71.0	1.72	52.6
34.3	42.0	0.340	496	77.0	2.27	52.5
26.3	41.5	0.560	431	79.0	1.70	46.4
28.5	26.5	0.540	465	62.0	1.82	47.0
26.7	30.0	0.550	545	84.0	2.25	75.4
36.1	44.0	0.550	609	112.0	2.20	72.6
27.3	47.5	1.230	728	130.0	3.35	115.3
29.2	28.0	1.260	740	140.0	3.45	120.3
			HSVA			
35.0	19.5	0.156	367	42.3	1.31	42.7
25.0	19.5	0.319	720	111.9	4.47	83.7
22.0	19.0	0.384	370	38.4	1.20	34.2
22.0	19.0	1.190	756	110.1	4.07	90.5
35.0	20.0	0.487	502	52.6	2.32	57.9
35.0	20.0	0.800	654	87.4	3.55	67.5
23.0	19.0	0.563	514	51.0	2.02	39.9
23.0	19.0	1.130	684	90.9	2.90	73.9
23.0	22.0	0.725	534	49.5	2.54	44.6
24.0	19.0	1.010	736	92.4	4.01	110.2
			JSRI			
21.5	21.3	0.122	262	20.0	0.58	17.1
21.5	21.3	0.553	442	44.5	1.51	30.9
23.0	19.3	0.783	516	53.1	2.13	49.1
21.7	23.4	1.230	730	101.9	3.79	64.5
37.4	37.2	0.112	384	45.7	1.22	50.2
37.4	37.2	0.561	636	82.1	3.87	75.2
23.1	30.4	0.108	266	20.5	0.53	21.2
23.1	30.4	0.550	479	49.3	2.12	35.9
35.5	34.9	1.230	881	150.0	6.78	156.9
23.3	42.7	1.230	787	119.8	5.11	95.9
22.1	42.6	0.783	570	69.5	2.51	50.1
22.2	40.8	0.112	298	25.6	0.67	21.7
22.2	40.8	0.335	383	39.5	1.12	25.9
36.0	40.7	0.783	698	101.5	4.84	95.6
34.6	50.5	1.006	895	157.9	6.14	121.7
23.5	37.9	1.007	713	121.7	4.27	72.7
37.9	38.3	1.008	932	135.4	6.02	123.2
21.7	22.8	0.335	301	21.5	0.54	22.5
21.7	22.8	1.010	721	110.9	3.62	62.0
			WARC			
24.0	18.0	0.130	305	29.2	1.10	22.1
22.0	15.0	0.580	474	55.0	1.50	32.6
25.0	21.0	1.240	775	125.0	2.50	120.6
25.0	21.0	0.580	467	52.0	1.40	42.
19.0	21.0	0.130	392	45.0	1.30	34.4
25.0	21.0	1.250	844	123.0	3.22	121.3
20.0	17.0	0.130	242	31.0	.22	4.
19.0	17.0	0.530	542	72.0	1.70	26.9
25.0	15.0	1.250	725	63.0	2.20	62.9

Table A2 (cont'd). Self-propulsion points of smooth model.
b. Nondimensional data.

F_n	C_a	J_t	K_t	$10K_q$	t
		CRREL			
0.21	125.0	0.11	0.387	0.365	0.21
0.21	90.0	0.11	0.391	0.367	-0.29
0.18	61.0	0.09	0.305	0.373	0.22
0.13	14.0	0.08	0.295	0.375	0.17
0.52	69.0	0.19	0.399	0.346	0.25
0.69	128.0	0.20	0.310	0.405	0.31
1.12	151.0	0.33	0.328	0.342	0.41
1.22	35.0	0.34	0.295	0.362	0.24
0.89	79.0	0.23	0.383	0.368	0.29
0.92	124.0	0.26	0.302	0.419	0.34
1.38	177.0	0.49	0.245	0.327	0.10
1.42	121.0	0.50	0.255	0.305	0.14
		HSVA			
0.27	57.0	0.12	0.314	0.472	0.04
1.42	57.0	0.33	0.216	0.416	0.02
0.43	83.0	0.30	0.262	0.425	0.07
1.55	55.0	0.46	0.193	0.346	0.07
0.33	53.0	0.39	0.209	0.447	-0.10
1.37	51.0	0.35	0.204	0.402	-0.20
1.40	54.0	0.38	0.193	0.371	0.02
1.33	44.0	0.48	0.173	0.301	0.03
1.83	38.0	0.40	0.174	0.422	0.12
1.75	57.0	0.40	0.170	0.399	-0.19
		ISRI			
0.27	101.0	0.14	0.291	0.410	0.15
1.22	101.0	0.36	0.229	0.400	0.21
1.55	86.0	0.44	0.199	0.366	0.29
1.57	110.0	0.49	0.191	0.345	0.17
0.17	101.0	0.08	0.310	0.401	-0.12
0.93	101.0	0.25	0.203	0.454	0.27
0.33	134.0	0.12	0.290	0.363	-0.02
1.16	134.0	0.33	0.215	0.449	0.27
1.08	100.0	0.41	0.193	0.424	-0.25
1.57	187.0	0.46	0.193	0.400	0.22
1.68	196.0	0.40	0.214	0.375	0.29
0.24	187.0	0.11	0.299	0.355	0.19
0.72	187.0	0.25	0.259	0.272	0.32
1.32	115.0	0.33	0.208	0.462	0.05
1.72	149.0	0.33	0.209	0.193	0.27
1.03	163.0	0.41	0.200	0.408	0.19
1.55	103.0	0.32	0.213	0.504	0.03
0.73	107.0	0.32	0.238	0.342	-0.25
[illegible]	107.0	0.41	0.213	0.339	0.47
		WARC			
0.21	75.5	0.12	0.312	0.474	N.A.
1.15	63.4	0.38	0.245	0.345	N.A.
1.62	49.6	0.47	0.175	0.222	N.A.
[illegible]	125.4	0.26	0.233	0.311	N.A.
0.26	26.4	0.10	0.333	0.410	N.A.
1.62	86.6	0.43	0.16	0.324	N.A.
0.19	76.5	0.11	0.266	0.420	N.A.
1.27	91.0	0.32	0.244	0.262	N.A.
1.62	106.2	0.57	0.139	0.225	N.A.

Table A3. Resistance test results with roughnened model.

a. Dimensional data.

h_i (mm)	σ_f (kPa)	V (m/s)	R_{it} (N)
CRREL			
22.0	26.0	0.110	22.0
17.0	20.0	0.342	37.0
19.5	20.0	0.574	40.0
24.0	24.0	0.780	57.0
19.0	25.0	1.016	87.0
23.0	26.0	1.220	37.0
25.0	21.0	0.233	43.0
22.0	27.0	0.782	60.0
24.0	24.0	1.256	97.
22.0	22.0	0.327	25.7
26.0	20.0	0.554	54.0
24.0	21.0	0.997	59.4
36.0	27.0	0.118	43.2
27.0	29.0	0.340	47.0
32.0	32.0	0.570	70.5
31.0	35.0	0.799	75.0
34.0	33.0	1.050	110.9
29.0	27.0	1.233	105.0
33.0	40.0	0.110	29.0
25.0	35.0	0.795	56.0
34.0	40.0	1.227	92.0
42.0	45.0	0.115	77.0
40.0	45.0	0.356	86.0
40.0	45.0	0.524	123.0
37.0	40.7	0.792	122.0
36.0	50.0	1.002	134.0
35.0	50.0	0.553	90.0
41.0	43.0	0.129	84.0
44.0	55.0	0.561	144.0
42.0	47.0	0.331	98.0
HSVA			
22.5	22.0	0.560	51.0
22.0	20.0	0.340	25.0
22.5	20.0	0.110	22.0
22.5	20.0	1.220	149.0
32.5	24.0	0.560	72.0
31.5	21.0	0.340	54.0
31.0	21.0	0.110	22.0
22.5	38.0	1.220	122.0
23.0	42.0	0.560	45.0
22.5	39.0	0.340	27.0
22.0	39.0	0.110	25.0
34.0	44.0	1.220	189.0
35.0	43.0	0.560	92.0
34.0	40.0	0.340	57.0
34.0	42.0	0.110	51.0
JSRI			
21.9	22.2	0.112	18.2
21.8	21.6	0.559	45.3
21.5	21.6	0.783	60.0
21.9	22.3	1.030	80.7
22.1	37.3	0.112	20.6
22.0	30.0	0.335	38.1
21.8	44.1	0.559	57.3
21.6	44.1	0.783	70.5
22.0	30.0	1.006	81.7
22.1	37.3	1.230	109.0
34.7	38.3	0.112	65.3
35.8	39.4	0.335	92.4
34.7	46.9	0.559	116.3
JSRI Continued			
34.7	46.9	0.783	[illegible]
35.8	31.4	1.006	[illegible]
34.7	39.3	1.230	[illegible]
36.4	22.9	0.112	[illegible]
35.1	34.4	0.335	40.2
34.9	22.1	0.559	87.1
34.9	39.1	0.783	116.0
35.1	34.5	1.006	128.5
36.4	22.9	1.230	173.6
[illegible]			
25.9	35.1	[illegible]	28.9
25.7	26.4	[illegible]	51.0
25.4	26.7	0.553	51.5
25.8	25.6	0.780	62.7
23.8	23.4	0.996	88.9
25.0	23.7	1.226	[illegible]
37.0	35.6	0.116	67.7
38.1	38.6	0.336	87.3
33.0	39.0	0.558	[illegible]
36.8	35.6	0.776	[illegible]
38.0	40.4	0.998	45.0
39.0	39.9	1.227	[illegible]
NRCC			
34.4	40.0	0.102	59.0
34.0	42.0	0.500	129.0
34.0	40.0	0.850	95.0
36.1	40.0	1.250	98.0
[illegible]	43.0	0.100	33.0
34.0	43.0	0.500	61.0
32.8	43.0	0.850	81.0
33.5	43.0	1.250	113.0
25.0	22.0	0.100	23.0
24.9	22.0	0.500	56.0
23.5	22.0	0.850	75.0
22.6	22.0	1.250	102.0
25.8	22.0	0.500	74.0
25.2	22.0	0.850	99.0
25.4	22.0	1.250	158.0
WARC			
22.0	21.7	0.110	36.0
20.0	24.0	0.110	29.6
25.0	21.0	0.110	56.9
26.5	17.8	0.560	104.6
25.9	16.7	0.800	[illegible]
22.9	27.0	0.110	51.6
22.2	18.5	0.560	115.2
22.4	22.0	0.800	162.2
30.2	34.9	0.110	32.0
30.2	35.3	0.560	71.2
30.1	34.8	0.800	99.5
36.3	39.3	0.110	45.2
34.6	45.9	0.110	95.5
34.7	43.3	0.560	144.7
33.5	46.0	0.800	158.7
33.5	39.5	0.110	72.2
32.2	39.6	0.560	117.6
32.7	34.	0.800	159.1

Table A3 (cont'd). Resistance test results with roughnened model.
b. Nondimensional data.

F_n	C_n	$R_{it}/\gamma B h_i^2$	$R_i/\gamma B h_i^2$
CRREL			
0.24	129.7	5.30	4.35
0.64	73.3	9.84	9.18
1.31	104.6	11.06	9.71
1.61	101.3	12.25	10.50
2.25	134.1	18.34	15.14
2.59	116.2	18.21	14.32
0.71	82.2	5.72	5.33
1.68	125.1	12.12	11.12
2.53	101.8	17.75	13.55
0.72	80.7	7.75	7.26
1.12	79.4	8.46	7.71
2.06	89.2	10.69	10.02
0.20	75.5	3.92	3.90
0.66	129.5	5.75	5.52
1.02	95.5	7.28	5.79
1.43	92.2	8.32	7.31
1.91	82.9	10.10	8.52
2.32	94.9	13.52	10.86
0.22	177.3	5.77	5.72
1.61	142.7	11.12	9.54
2.55	158.9	16.32	12.75
0.19	114.7	5.07	5.04
0.57	114.7	6.21	5.18
0.84	114.7	8.12	7.31
1.31	112.2	9.45	8.74
1.69	141.6	10.33	9.68
0.34	174.7	7.74	7.33
0.17	124.4	5.61	5.59
0.65	123.7	7.83	7.56
1.54	114.1	11.22	10.35
HSVA			
1.17	95.4	9.70	9.32
0.72	96.6	6.95	6.61
0.23	90.6	4.57	4.53
2.19	87.8	14.32	12.65
0.99	75.3	6.96	6.50
0.61	66.0	5.72	5.54
0.20	69.1	3.50	3.49
2.60	172.2	25.33	20.86
1.19	186.1	9.73	8.91
0.72	176.7	7.66	7.32
0.23	172.8	4.97	4.92
2.13	131.9	17.19	15.20
0.96	125.2	7.99	7.49
0.59	119.9	6.09	5.92
0.19	125.9	4.64	4.62
JSRI			
0.24	106.6	4.00	3.95
1.22	102.4	10.32	9.25
1.70	102.4	13.56	11.51
2.65	106.6	20.35	15.52
0.24	164.6	6.04	5.99
0.72	139.0	9.29	7.91
1.21	208.1	12.34	11.87
1.72	208.1	15.91	13.65
2.17	139.2	17.79	14.55
2.56	164.6	21.61	17.15
0.19	112.5	5.76	5.73
0.57	112.2	7.93	7.44
0.96	107.8	10.17	9.75
JSRI (Continued)			
1.34	97.6	11.65	10.75
1.72	112.2	12.42	11.19
2.11	112.5	14.45	12.61
0.19	92.1	4.77	4.74
0.57	90.1	6.87	6.77
0.95	102.5	8.42	7.98
1.34	102.5	12.21	9.41
1.71	121.1	11.92	10.65
2.05	92.1	13.78	12.07
NKK			
0.23	142.1	6.11	6.07
0.67	144.4	8.12	7.65
1.12	147.2	8.57	7.80
1.55	144.6	9.92	8.43
2.06	168.0	15.34	13.15
2.47	150.2	19.77	15.06
0.19	97.3	5.15	5.12
0.55	103.3	6.26	6.24
0.91	104.8	8.16	7.80
1.29	98.5	9.27	8.57
1.53	107.8	10.52	9.47
1.98	104.3	12.29	10.75
NRCC			
0.17	118.9	5.25	5.23
0.97	113.9	9.93	9.57
1.47	116.9	14.23	13.25
2.10	112.9	15.84	13.89
0.21	181.9	5.98	5.94
1.03	182.6	11.15	10.45
1.80	192.2	16.41	14.24
2.50	186.5	22.69	19.75
0.20	89.7	4.89	4.85
1.01	90.1	9.35	9.20
1.77	95.4	14.30	12.26
2.60	95.0	19.29	14.39
0.84	65.5	6.09	5.75
1.45	66.6	8.33	7.42
2.12	66.2	13.28	11.36
WARC			
0.23	96.2	7.15	7.11
0.25	120.5	7.55	7.50
0.19	60.6	4.90	4.78
0.94	48.9	9.84	9.48
1.35	53.1	14.03	13.27
0.19	63.7	5.01	4.99
0.98	60.0	10.93	10.49
1.42	72.4	16.35	15.41
0.25	175.3	8.16	8.11
1.25	177.3	18.16	16.97
1.80	176.5	25.55	23.21
0.21	151.4	6.76	6.73
0.19	138.2	7.59	7.58
0.97	148.7	13.00	12.58
1.40	140.0	15.80	14.92
0.19	119.8	6.53	6.52
1.00	94.3	12.07	11.59
1.41	106.3	15.24	14.32

Table A4. Self-propulsion points of roughnened model.

a. Dimensional data.

h_i *(mm)*	σ_i *(kPa)*	V *(m/s)*	n_a *(rpm)*	T_a *(N)*	Q_a *(Nm)*	R_p *(N)*
			CRREL			
38.0	45.0	0.340	520	115.0	2.01	90.1
31.0	45.0	0.520	543	111.0	2.43	82.4
37.0	32.0	0.740	744	133.0	4.71	115.7
25.0	25.0	0.520	497	65.0	2.02	49.4
26.0	26.0	0.750	610	82.0	3.05	69.2
22.0	33.0	1.200	786	122.0	4.79	93.2
			JSRI			
20.5	40.0	0.112	316	30.8	0.84	30.2
22.2	48.4	0.335	441	55.9	1.50	46.8
22.1	28.9	0.559	511	66.4	2.10	46.2
21.4	32.6	0.783	584	77.6	2.68	59.4
22.3	34.9	1.006	680	95.5	3.64	80.0
22.0	40.9	1.230	792	123.0	4.86	103.4
35.0	44.0	0.112	479	74.7	1.34	63.5
35.0	44.0	0.559	643	119.8	4.19	99.4
33.1	40.6	0.783	711	132.3	4.84	111.7
35.4	37.1	1.230	954	206.0	9.13	178.8
			NRCC			
36.0	32.0	0.609	720	121.8	5.06	97.0
36.0	32.0	0.339	584	95.8	2.85	71.5
24.0	16.0	0.601	530	62.3	2.46	46.0
24.0	16.0	0.508	478	50.7	2.03	40.4
25.0	20.0	1.113	684	93.1	3.65	92.4
25.0	20.0	1.243	798	130.0	4.86	105.2

b. Nondimensional data.

F_n	C_n	J_a	K_t	$10K_q$	t
		CRREL			
0.56	120.7	0.16	0.302	0.380	0.22
0.94	148.0	0.24	0.268	0.403	0.26
1.23	88.2	0.29	0.240	0.413	0.13
1.05	101.9	0.30	0.263	0.397	0.24
1.49	101.9	0.36	0.220	0.398	0.16
2.58	152.9	0.44	0.197	0.375	0.24
		JSRI			
0.25	198.3	0.10	0.308	0.407	0.02
0.72	222.2	0.22	0.287	0.374	0.16
1.20	133.3	0.32	0.254	0.390	0.30
1.71	155.3	0.39	0.227	0.382	0.23
2.15	159.5	0.43	0.207	0.382	0.15
2.65	189.5	0.45	0.196	0.376	0.16
0.19	128.1	0.07	0.325	0.409	0.15
0.95	128.1	0.25	0.290	0.492	0.17
1.37	125.0	0.32	0.262	0.464	0.15
2.09	106.8	0.38	0.226	0.487	0.13
		NRCC			
1.02	90.6	0.25	0.235	0.475	0.20
0.57	90.6	0.17	0.281	0.405	0.25
1.24	68.0	0.33	0.222	0.425	0.26
1.05	68.0	0.31	0.222	0.431	0.20
2.25	81.5	0.47	0.199	0.379	0.01
2.51	81.5	0.45	0.204	0.370	0.19